27(1-2)

27(1-2

気象庁欧文海洋報告

第27巻 第1-2号

THE OCEANOGRAPHICAL MAGAZINE

Vol. 27 No. 1-2

LIBRARY
SEP 27 1977
FISH & WILDLIFE SERVICE

CONTENTS

ISOZAKI, I., T. UJI, T. SETO and A. KAIETSU: Ocean waves on Sagami Bay caused by Typhoon 7416 1

NAGASAKA, K.: Direct measurement of deep-sea current by Richardson-type current meters in the western-north Pacific 25

ISEZAKI, N.: A preliminaay report of magnetic survey in GDP; Geomagnetic anomaly lineation in the area southwest of Shatzky rise 37

UEDA, F.: On the quality control of marine meteorological data practiced in Japan Meteorological Agecy 43

Published by the Japan Meteorological Agency

March, 1976

投稿規定

1　資　格

原則として，気象庁職員に限る。ただし，気象庁職員との連名の場合は，この限りでない。

2　論文及び報文（以下「論文等」という。）の内容

未発表の原稿で，海洋（物理・化学・生物・地質など）及び海上気象（波浪・海水・海気相互関係など）に関する論文並びに気象庁における海洋・海上気象業務の活動，そのために開発された測器及び方法に関する報文など。

3　書き方

(1) 用語は，欧文（原則として英文）とする。

(2) 論文等には，英文（300語以内）及び和文（800字以内）の要約を受ける。要約は，方法・測器・実験・観測の結果・仮定・理論などの中味が読みとれるように留意し，なるべく指定の長さで簡潔に書く。

(3) 論文等の始めには，題名・著者名及所属機関名を明記する。和文の要約にも同様のことを明記する。

(4) 原稿は，厚手の用紙にダブルスペースでタイプする。

(5) 図は，白紙又は青方眼紙に墨入れし，図及び図中の文字の大きさは，印刷の際の縮小率を考えて作成する。特に重要な図は，投稿者が大きさを指定する（印刷の都合上，希望どおりにならないこともある。）

(6) 図（写真を含む。）及び表には，必ず説明を付ける。図の説明文は，別紙にタイプする。折り込みの図及び表は，なるべく避ける。図及び表のそう入箇所を本文の欄外に記入する。

(7) 数式は，2行取りに書き，数式の文字及び記号をはっきりと説明する。

(8) 論文等の中に文献を引用する場合は，「Allen (1927)」又は「(Allen, 1927)」のように書く。

(9) 引用文献は，最後にまとめて付け，著者名のアルファベット順に並べる。書き方は次のようにする。

Allen, W.E. (1927): Surface catches of marine diatoms and dinoflagellates made by U.S.A. Pioneer in Alaskan waters in 1923. *Bull. Scripps Inst. Occanogr., Tech. Ser.* **1**(4), 39-48.

Budyko, M.I. (1956): *The heat balance of the earth's surface*. Hydrometeorogical Publishing House, Leningrad, pp. 254.

Veronins, G. and H. Stommel (1956): The action of a variable wind stress on a stratified ocean. *J. Mar. Res.*, **15**(1), 43-75.

4　提出方法

投稿票を付け，本稿のほかにコピー（図及び表を含む。）2部を添える。

5　締切り

毎年気象庁公報により公示する。

6　送付先

気象庁海洋気象部海洋課

（原則として，書留便で送付する。）

7　その他

論文1等編につき別刷り50部を著者に無料で送付する。

Oceanographical Magazine

編集委員長　Editor

安井　正，M. YASUI

編集委員　Editorial Board

飯田　隼人，H. IIDA*
磯崎　一郎，I. ISOZAKI**
小長　俊二，S. KONAGA**
猿橋　勝子，K. SARUHASHI**
伊勢崎　修弘，N. ISEZAKI***
川原田　裕，Y. KAWARADA***
中野　旭，A. NAKANO*
鈴置　哲朗，T. SUZUOKI*

* 気象庁 JAPAN METEOROLOGICAL AGENCY

** 気象研究所 METEOROLOGICAL RESEARCH INSTITUTE

*** 気象大学校 METEOROLOGICAL COLLEGE

The Oceanographical Magazine
Vol. 27, Nos, 1-2, pp. 1 to 23, March 1976

Ocean Waves on Sagami Bay Caused by Typhoon 7410

Ichiro ISOZAKI and Takeshi UJI
Meteorological Research Institute

Tsutomu SETO and Akira KAIETSU
Tokai Univeasity

(Received August 27, 1975)

Abstract: Swells ovserved off Hiratsuka on the coast of the innermost part of Sagami Bay and off Habu-harbor on the southwestern end of Oshima Island situated on the mouth of the bay during the passege of Typhoon 7416 are presented in the Paper.

Wave heights observed at Hiratsuka are about 40% lower than those at Habu-harbor in average, but their time variations are almost similar to each other. Numerical experiments showed that the above-mentioned differences of wave heights between the two stations are largely due to the sheltering effect of peninsulas and island. It is surprising that the swell caused by Typoon 7416 reached the coast of Hiratsuka from the bay mouth suffering wave height reduction of about 30%, in spite of southeasterly swell direction from which the swell incidented upon Sagami Bay normally.

In conclusion, we emphasize that wave observations near coasts may be used effectively to supplement the lack of wave data on the ocean, after careful procedures to correct wave distortion due to sheltering, shoaling, refraction, diffraction, reflection and several processes of energy dissipation.

1. Introduction

A number of numerical models of ocean wave prediction have been proposed in the last ten years stimulated by the progresses of theoretical studies of ocean wave generation and the development of powful electronic computer. They are GELCI and DEVILLAZ (1970), PIERSON, TICK and BAER (1966), INOUE (1967), BARNETT (1968), BARNETT, et al. (1969), EWING (1971), and ISOZAKI and Uji (1973, 1974). These models can be described unficatively by means of the radiative transfer equation. Source functions contained in the equations of respective models, however, have different types owing to the adoption of different physical assumptions. Nevertheless, as shown by GELCI and DEVILLAZ (1970) and DEXTER (1974), the differences in the predicted results of respective models are relatively slight.

In the introduction of these modern techniques into routine operation of wave forecesting demonstrating their superiority, three problems have to be solved:

(1) forecasting accurately wind, in both space and time, at any desired height above the mean sea level,

(2) expressing adequately the wind and wave fields in typhoon and severe strom areas,

(3) accumulating wind and wave data over the ocern.

The first problem is very important, because the reliability of ocean wave prediction depends critically on the accuracy of surface wind estimation. It has long been cosidered that the estimation of wind in the atmospheric surface boundary layer is very difficult because of its large variability in both space and time. Accordingly, most of practical techniques for predicting ocean surface winds have depended on empirical and statistical methods. Methods multiplying the gradient wind speed by the empirical correction factors in relation to the atmospheric stability and the roughness of sea surface are used commonly.

On the other hand, recent advances in the investigation of atmospheric turbulence have led to a great confidence in specifying the vertical distribution of wind and temperature in the marine atmospheric boundary layer. CARDONE (1969) developed a simple two- layer model of the marine atmospheric boundary layer which includes effects of atmospheric stability and baroclinicity. Isozaki and UJI (1974) examined Cardone's model concerning its operational usage, and concluded that the model can be applied to prepare appropriate wind information for the wave forecasting. Now the Japan Meteorological Agency is testing the model extensively for the purpose of introducing it into routine operation.

The second is purely thechnical problem. Waves caused by a typhoon dominate the sea state remarkably not only within a typhoon area but also exert significant influence on the coast more than 1000 km away from the typhoon. In the operation of a numerical wave prediction model, mesh size larger than a handred kilometers and a time step of several hours are usually adopted because of the low accuracy of wind estimation and economy in the use of an electronic computer. Distribution of winds and waves in a typhoon area will not be represented precisely with such rough meshes. Therefore, some new devices must be made to predict the waves in a typhoon area. As one of provisional ways we are going to establish a experimental formula based on a number of numerical tests.

The third problem is verh important not only for verification of wave prediction but also for improvement of numerical models. The above-metioned numerical

models of ocean wave prediction should be modified cosidering the recent advance in theoretical studies, especially on the wave-wave interation and the mechanism of air-sea momentum transfer. It is assumed that several nonlinear mechanisms will control strongly growth and dissipation processes of the ocean waves under gale conditions. But the actualities are not known owing to scantiness of reliable wave data taken under such conditions. Very high waves in a typhoon area have been investigated by many authors because of their significant influence on transport, fishing and mining activities, but most of their results have never been confirmed by observation.

Some of the wave data taken at oceanographic observation tower may be utilized to supplement the lack of wave data on the ocean. Of course the data taken near coast are distorted by the influence of bottom and coastal topographies. If we can relate the wave characteristics observed near coast to the one taken offshore deep waters through the investigations of topographic influence, the coastal wave observetions will become important incresingly.

In this paper, wave data taken at the Oceanograpic Observation Tower, Hiratsuka, especially the waves caused by Typhoon 7416, are analysed, and compared with the waves observed off Habu-harbor, Oshima Island. The differences of wave height between the two stations are convenient to discuss the modification of wave characteristics during the propagation of offshore deep water waves into coastal region, because the waves in consideration were swell and affected by breeze or moderate winds during the passage over Sagami Bay.

2. Shoaling and refraction

Details of wave modification due to bottom topography when short-crested irregular waves propagate into shallow water are still not well known. And the assumptions adopted here as a matter of conveniece are that the waves are composed of a number of long-crested small-amplitude sinusoidal wave components and each wave components behaves independently.

There are a number of effects which modify the wave characteristics in shallow water region: they are the sheltering by cape and peninsula, the shoaling, the refraction, the diffraction, the reflection and many processes of energy dissipation. The Oceanographic Observation Tower of the Institute of Coastal Oceanography, National Research Center for Disaster Prevension, Hiratsuka, Japan, where we have made wave observations from Aug. 30 to Sept. 30, 1974, is at a point about 1000 meters from the coast of Sagami Bay (lat. 35°18.1′ N, long. 139°20.8′ E). The coast

line and bottom contours near the tower extend monotonously from west to east, and the water depths there are about 20 meters. Accordinly, it is sufficient to consider only the effets of the sheltering, and the refraction in the analysis of wave data taken at the tower.

If the wave energy contained between orthogonals remains constant with no reflection of energy from the varying water depth and no gain or loss of energy by the processes as the wave front progresses, the variation of wave height in a shallow water region is, as seen in usual text books of physical oceanography, represented as

$$\frac{H}{H_0}=\left(\frac{b_0}{b}\right)^{1/2}\left(\frac{1}{2n}\frac{C_0}{C}\right)^{1/2}=K_r\cdot K_s \tag{2.1}$$

where

$$K_r=\left(\frac{b_0}{b}\right)^{1/2}\quad,\quad K_s=\left(\frac{1}{2n}\frac{C_0}{C}\right)^{1/2} \tag{2.2), (2.3}$$

are the refraction coefficient and the shoaling coefficient respectivery, where

$$\frac{C_0}{C}=\frac{L}{L_0}=\tanh\,(2\pi h/L) \tag{2.4}$$

$$n=\frac{1}{2}\left[1+\frac{4\pi h/L}{\sinh\,(4\pi h/L)}\right] \tag{2.5}$$

Here, H, C, and L are the wave height, the wave speed and the wave length at a depth of h, and H_0, C_0, and L_0 the wave height, the wave speed and the wave length in deep water respectively. b_0 and b are the widths between orthogonals in deep and shallow water respectively.

Variations of shoaling coefficient at the water depth of 10, 20, 40, 60, 120 and 140 meters are shown in Figure 1 as a function of wave period. It is seen that waves with period less than 16 sec do not feel the bottom and behave as deep water waves at the 200 meter-depth. Near the Oceanographic Observation Towr, Hiratsuka where the water depth is about 20 meters, the waves with periods less than 4 sec behave as deep water waves, the waves with periods between 5 sec and 14 sec have shoaling coefficients less than unity (minimum of them is 0.912 for the waves with period of 9 sec), and the waves with periods more than 16 sec have coefficients larger than unity. Accordingly the heights of usual wind waves and swell observed at the Tower, Hiratsuka are lower than the heights of offshore deep water waves due to shoaling effect.

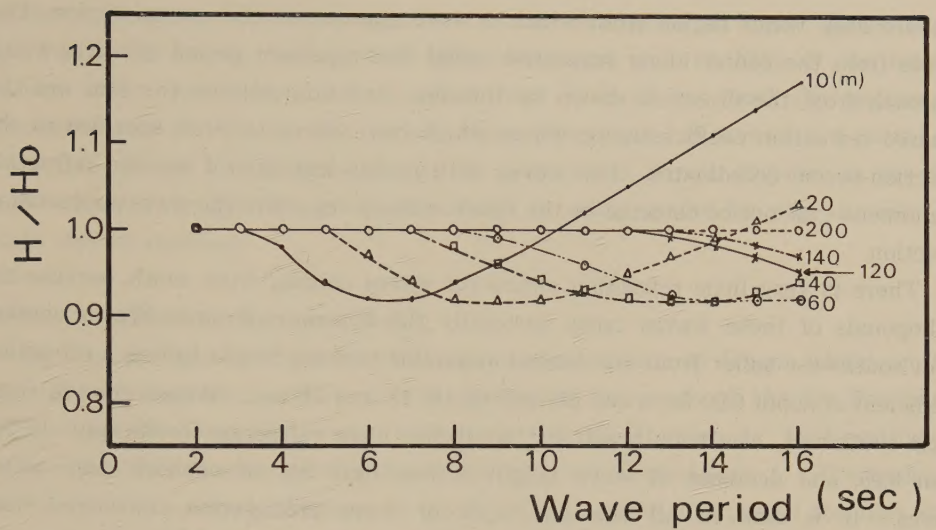

Fig. 1. Relation between shoaling coefficient and wave period for several fixed water depths.

When a wave propagates into a shallow water region, the wave ray refracts according to the depth variation because a wave velocity is a function of water depth. It is confirmed by observations that the way of refraction is conformed to the Snell's law similar to the refraction in the geometric optics. Practically, the refraction coefficient is estimated from values of b and b_0 obtained directly from the construction of a refraction diagram.

There are several methods of constructing a refraction diagram which may be classified into two groups: orthogonal method and wave front method; the graphical techniques of the former method developed by ARTHER, MUNK and ISSACS (1952) is generally used in Japan. Here we adopted a numerical method proposed by WILSON (1966) wich calculates a wave ray by use of electronic computer and draws it on a plotter directly. The method is very convenient to make a number of refraction diagrams in a short time. In the present investigation, twenty-five refraction diagrams were costructed for waves which approach the coast of Hiratsuka from southwest, south-southwest, south, south-southeast and southeast with wave periods 4, 7, 10, 13 and 16 sec respectively, and refraction coefficients near the Tower are estimated for each wave.

Fig. 2 shows squared values of the coefficient obtained above. In the figure lines stretched radially from the center of semi-circle are the orientation on the

offshore deep water region from which a wave approaches the coastal region. Distances from the center along respective radial line represent period of waves which approach from the direction shown by this line, and numerals on the line are the squared refraction coefficients for waves which have characteristics specified in the direction-period coordinates. For waves with perods less than 4 sec, the refraction phenomena can not be detected in the figure without regard to the wave approaching direction.

There is very little refraction effects for waves coming from south, because the orthogonals of these waves cross normarlly the bottom contours. Waves coming from southwest suffer from the largest reduction of wave height having a refraction coefficient of about 0.90 for wave periods of 10, 13 and 16 sec. Waves coming from south-southwest, south-southeast and southeast have refraction coefficients larger than 0.95, and decrease of wave height is less than 5% of offshore deep water waves. It is seen in all the directions of wave propagation considered here that the refraction coefficient decreases with increasing wave period.

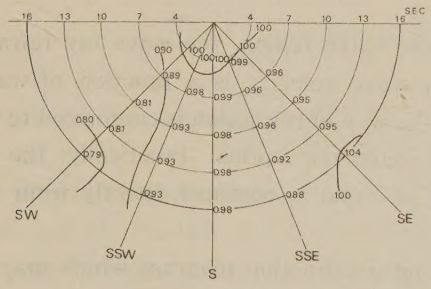

Fig, 2. Squared refraction coefficient near the Oceanographic Observation Tower, Hiratsuka for waveswith different periods and travel directions.

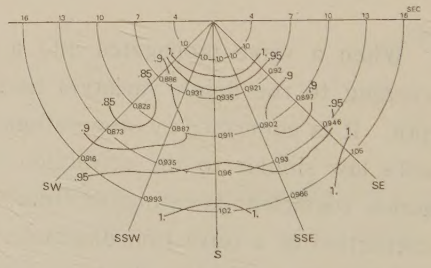

Fig. 3. Combined effect of the shoaling and the refraction near the Oceanographic Observation Tower, Hiratsuka for waves with different periods and travel directions.

Fig. 3 shows combined effects of the shoaling and the refraction ($K_r \cdot K_s$) represented by Equation (2.1). The construction of the figure is the same as Fig. 2. The figure shows that waves with periods less than 5 sec do not change their height from the initial values in the offshore deep water area even if they approach from any direction. Waves coming form southwest suffer from the wave height reduction of about 10 to 18% of the height of deep water waves offshore, and the

maximum decrease of 18% is seen for waves with period of 9 sec. Decrease of wave height for waves coming from other directions is 5 to 10% of the height of deep water waves in a period range from 7 to 13 sec, and the maximum decrease is seen for waves with periods about 10 seconds. Waves with a period of 16 sec have almost the same height as the deep water waves offshore, as the decrease of wave height due to the refraction is compensated by the increase of height due to shoaling.

3. Waves caused by Typhoon 7416

As seen in Fig. 4, Typhoon 7416 was on the sea east off Guam Island on 26, Aug. 1974 moving north-northwest, and reached 440 km south off the Izu Peninsula at 21^h, Aug. 30. Then the typoon turned the travel direction to west-northwest and reached 200 km south off Shikoku on the early morning of Sept. 1. The typhoon again turned the travel direction to north at that point and passed through Shikoku and Chugoku after landing on the coast near Kochi, Shikoku at 18^h 20^{min}, Sept. 1.

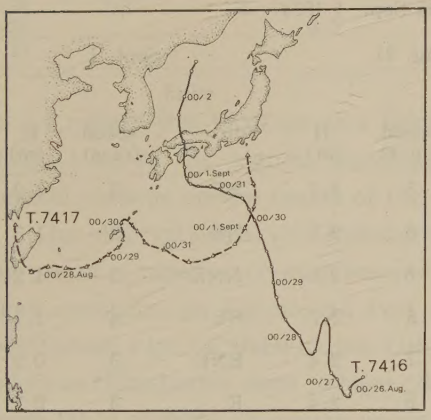

Fig. 3. Trajectory of Typhoon 7416.

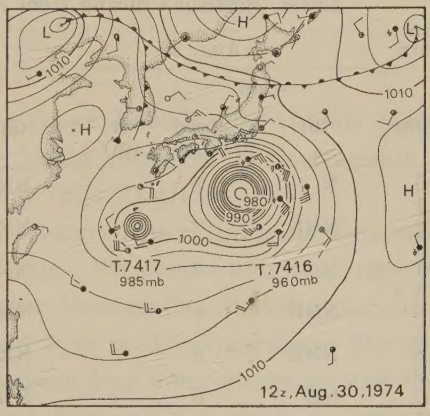

Fig. 5. Surface weather map at 12z, Aug. 30, 1974.

Fig. 5 shows a weather map at 21^h, Aug. 30, when the tyhoon was at 30.1°N, 139.9°E with a minimum atmospheric pressure of 960 mb and the maximum wind velocity of 35 m/s. This typhoon was one of the largest ever coming to Japan, and heavy rain associated with the typhoon caused severe damage to West Japan and the Kanto District. Huge waves attacked the Pacific coast of Japan, the highest

wave height of which seems to exceeded 10 meters near the landing point of the typhoon. The coasts of the Kanto and Tokai Districts, several hundreds kilometers away from the tyhoon track, were also attacked by huge swell, and a wave height

Table 1 Highest significant wave height observed at respective stations along the coasts of the Kanto and Tokai Districts during from Aug. 30 to Sept. 1, 1974

Station	Max. of $H_{1/3}$		Date	Wave gage	
	height (meter)	period (sec)		type (*)	depth (meter)
Hiratsuka	3.0	14.3	22^h, Aug. 30	CW	20
Habu-harbor	5.4	12.7	0^h, Aug. 31	USW	40
Shimizu-harbor	2.9	13.8	8^h, Aug. 31	USW	10
Oigawa-harbor	2.5	14.5	22^h, Aug. 30	PW	9
Omaezaki	5.0	13.8	22^h, Aug. 30	USW	13.5
Kashima	2.9	12.7	22^h, Aug. 30	USW	20

(*) CW : Capacitance-wire wave recording gage
USW: Ultra-sonic wave recording gage
PW : Pressure-type wave recording gage

Table 2 Significant wave heights and winds observed at the Oceanographic Observation Tower, Hiratsuka during from Aug. 30 to Sept. 1 1974

Date	Aug. 30			Aug. 31			Sept. 1		
	wind			wind			wind		
Time	dir.	speed (m/s)	H (m)	dir.	speed (m/s)	H (m)	dir.	speed (m/s)	H (m)
0	N	3		NNE	5	2.7	NE	3	1.2
1									
2	NNE	2		NNE	6	2.5	NE	3	1.3
3									
4	N	2		NNE	5	2.6	NNE	3	1.2
5									
6	NNE	4		NNE	5	2.7	NE	4	1.1
7									
8	NNE	6		NNE	7	2.4	ENE	3	0.9
9									
10	NE	6		NNE	5	2.4	E	3	0.7
11									
12	NNE	5		NE	7	2.4	ESE	3	1.0
13									
14	NE	4	2.0	NE	5	1.9	S	0	0.8
15									
16	E	5	2.6	NF	3	1.7	SE	0	1.0
17									
18	NNE	3	2.2	NF	4	1.8	SE	2	1.0
19									
20	NNE	2	2.5	NE	3	1.7	NNE	2	1.0
21									
22	NNE	3	3.0	ENE	3	1.2	N	1	1.2
23									

Table 3. Significant wave heights and winds observed off Habu-harbor, Oshima Island during from Aug. 30 to Sept. 1, 1974

Date	Aug. 30			Aug. 31			Sept. 1		
	wind			wind			wind		
Time	dir.	speed (m/s)	H (m)	dir.	speed (m/s)	H (m)	dir.	speed (m/s)	H (m)
0	NE	2	2.1	NE	3	5.4	E	2	2.9
1									
2			2.2			4.9			2.5
3	NE	2		NE	3		ENE	2	
4			2.1			4.6			2.2
5									
6	NE	2	2.5	NF	3	4.3	E	1	2.2
7									
8			2.7			5.0			2.3
9	N	2		NNE	3		E	1	
10			3.0			4.6			2.1
11									
12	NE	2	3.3	NE	3	3.8	ESE	1	2.2
13									
14			3.4			3.4			2.1
15	E	2		NNE	2		SE	1	
16			4.1			2.9			1.9
17									
18	NE	2	3.9	NE	2	3.1	ESE	1	1.7
19									
20			4.0			3.5			2.1
21	NE	2		NNE	2		SE	1	
22			4.5			2.5			2.1
23									

of 5.4 meters was recorded at a point about 1 km off Habu-harbor, Oshima Island. Table 1 shows the highest significant wave height measured by instruments at several stations on the coasts of the kanto and Tokai Districts.

Our observations at the Oceanographic Observation Tower, Hiratsuka were made by use of a capacitance-wire wave-recording gage. For comparison, wave observations conducted by the Second Port and Harbor Construction Bureau, Japan at a point about 1 km off Habu-harbor, Oshima Island were used in the paper. The data taken at Habu-harbor seem to have characteristics of deep water waves, because they were taken at about 48 meters water-depth and 1 km off the coast by use of a ultrasonic wave-recording gage set on the sea bed.

Winds and significant wave heights observed at Hiratsuka and Habu-harbor from Aug. 30 to Sept. 1 are tabulated in Tables 2 and 3 respectively. The maixmum wave height at Hiratsuka, 3.0 m, appeared at 22^h, Aug. 30 when the typhoon was turning the traveling direction from north-northwest to west-northwest at about 400 km south off the Izu Peninsula. On the other hand, the maxium wave height at Habu-harbor reached 5.4 m at 00^h, Aug. 31. The height of waves at Hiratsuka

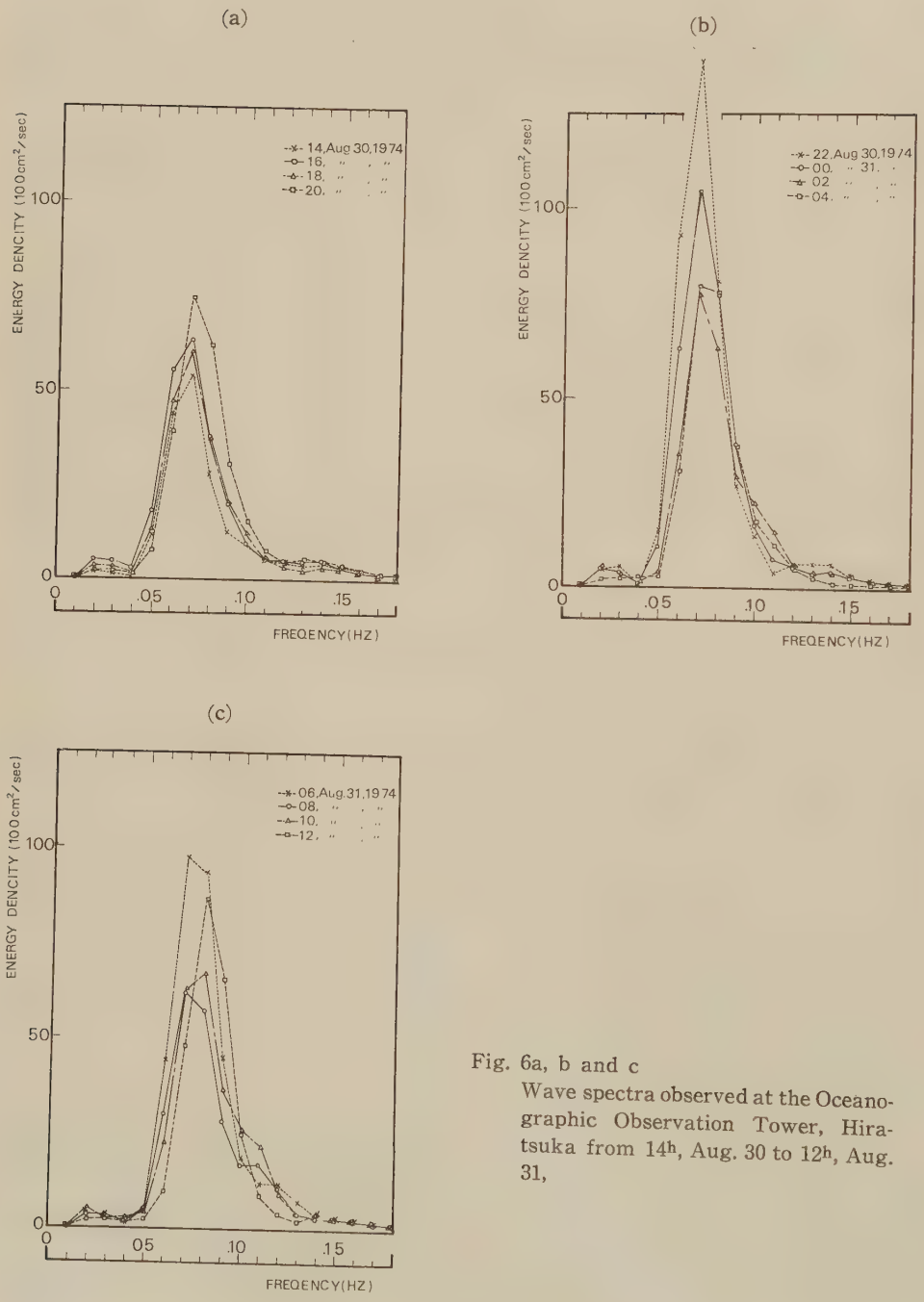

Fig. 6a, b and c
Wave spectra observed at the Oceanographic Observation Tower, Hiratsuka from 14h, Aug. 30 to 12h, Aug. 31,

is about 40% lower than the waves at Habu-harbor in average, but their variations are very similar to each other. In the present high wave period, winds were breeze or moderate over Sagami Bay, and the waves mentioned in these tables are swell entered in the bay from south. As has been discussed in the previous section, the large reduction of wave height at Hiratsuka cannot be explained by the shallow water effect. This will be discussed in the following section.

Figs. 6a, b and c show two-hourly wave spectra taken at Hiratsuka from 14^h, Aug. 30 to 12^h, Aug. 31. It is seen in these figures that the spectral density is growing up with time till the maximum energy level is reacehed at 22^h, Aug. 30, then begins to decay gradually. On the other hand, the frequency of spectral peak increases gradually with time, that is, peak frequency (period) is 0.067Hz (14.9 sec) between 14^h and 18^h, Aug. 30; 0.070Hz (14.3 sec) between 20^h Aug. 30 and 00^h, Aug. 31; 0.073Hz (13.7 sec) at 2^h, Aug. 31; 0.075Hz (13.3 sec) between 4^h and 10^h, Aug. 31; 0·080Hz (12.5 sec) between 12^h and 16^h, Aug. 31. The shift of spectral peak toward higher frequency continues further, and the wave spectra on the morning of Sept. 1 have energy peaks at the frequency (period) of 0.100Hz (10.0 sec). The waves mentioned here are the swell which was generated in the storm area of Typhoon 7416 and reached the coast of Hiratsuka after traveling several hundred kilometers. Accordingly, lower frequency (longer period) components which have faster travel speed are prevailing in the early stage of swell development, followed by the appearance of higher frequency (shorter period) components in the later stage of the development and the decay stage.

If the waves are assumed to propagate along a great circle on the ocean without bending due to currents and islands, most of the waves generated in a part of storm area where the wind direction is pointing to the coast of Hiratsuka within $\pm 30°$ could reach the coast after an appropriate travel time. Such storm area will be named "effective storm area" here. The effective storm areas are determined on each of six-hourly weather maps, and the distances of them from Hiratsuka are plotted on respective distance axes. Thus obtained six-hourly distance axes are placed along a time axis so as to construct a time-distance space. Then the effective storm area is determined on the time-distance space by drawing an envelope of storm distances on the succeeding distance axes. Fig. 7 shows the effective storm area of Typhoon 7416 in the time-distance space.

Now consider the spectrum at 22^h, Aug. 30 which has the highest energy level in this spectral series. It is shown in Fig. 6c that the large part of wave energy is concentrated in a narrow frequency band from 0.06Hz to 0.08Hz. Propagation

lines of frequency components 0.06Hz, 0.07Hz and 0.08Hz which have reached the coast of Hiratsuka at 22h, Aug. 30 are shown in Fig. 7. Crossing part of a propagation line to the effective storm area describes fetch and duration of the storm under which the wave component is excited For example, a wave component with frequency 0.07Hz grew up through the wind duration of 24 hours from 00h, Aug. 29 to 00h, Aug. 30 and the fetch of about 1000 km, went out the storm area at 00h, Aug. 30, then reached the coast of Hiratsuka as swell after traveling about 900 km.

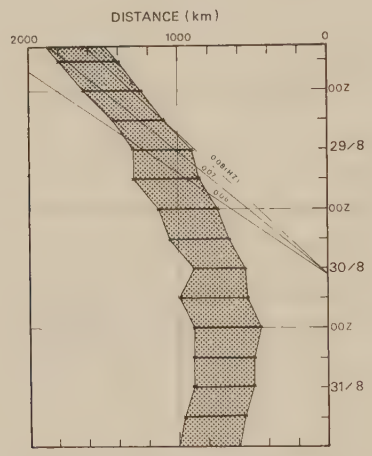

Fig. 7. Time-distance diagram showing the propagation of wave components. Shadow area is the effective storm area for waves observed on the coast of Hiratsuka.

The wave component with frequency 0.08Hz grew up through the duration more than 24 hours and the fetch more than 1000 km. These fetch and duration are sufficient for these wave components to reach the coast in a near fully developed stage. On the other hand, a wave component with a frequency of 0.06Hz is affected by about 12 hours-duration and 600 km-fetch. It is seen in Fig. 7 that frequency components lower than 0.06Hz are influenced by far less duration and fetch of the storm.

4. Numerical simulation of waves caused by Typhoon 7416

Numerical tests were conducted to understand some characteristics of the waves observed on the coast of Hiratsuka which are described in the previous section. Marine surface winds were computed by means of the numerical model developed by ISOZAKI and UJI (1974) Basic data used in the computation are sea-level atmos-

pheric pressure, surface air temperature and sea surface temperature Then wave spectra and wave heights are computed by use of the numerical model proposed by ISOZAKI and UJI (1973) based on the above-obtained marine surface winds.

4.1 Numerical model of marine surface winds

Actual surface winds are essentially turbulent and variable because of the critical influence of complex surface structure, atmospheric stability, etc. Especially on the marine surface, parameterization of the winds requires ultimately a knowledge of the process of wave generation because of the mutual exchange of the momentum between winds and waves. So the theoretical estimation of real surface winds is very difficult and empirical formula have been used for practical purposes.

Recently, BLACKADAR (1965) and CARDONE (1969) proposed a method of mariene surface wind estimation based on a theoretical model of atmospheric surface boundary layer. ISOZAKI and UJI (1974) confirmed the usefulness of the method and constructed a computation scheme for routine operation in the Japan Meteorological Agency. It is a two-layer baroclinic non-neutral model.

As seen in Fig. 8, the atmospheric surface boundary layer is assumed to be

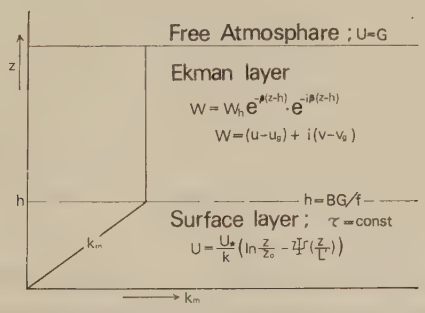

Fig. 8. Model of atmospheric surface boundary layer.

separated into two regions: surface layer and the Ekman layer. In the surface layer, the Coriolis parameter is neglected, the turbulent transfer coefficient for momentum (K_m) increases with height almost linearly, and the wind stress is constant. The vertical wind profile in this layer is represented as follows,

$$U_z=\frac{U_*}{k}\left[\ln\frac{z}{z_0}-\Psi(z/L')\right] \tag{4.1}$$

where U_z is the wind velocity at the height z, U_* the friction velocity, k the Karman constant, z_0 the roughness parameter, L' the modified stability length, and $\Psi(z/L')$

the correction term with respect to the atmospheric stability.

The height of the surface layer (h) is assumed to be specified explicitly in terms of the external parameters, and the Blackar's formulation,

$$h=B_0G/f \tag{4.2}$$

is adopted, where G is the gradient wind estimated from sea level atmospheric pressure, f the Coriolis parameter, and B_0 the constant. The effect of the wave motion on the structure of the surface wind is taken into consideration indirectly in the specification of the surface roughness parameter,

$$z_0=\frac{C_1}{U_*}+C_2U_*^2+C_3 \tag{4.3}$$

where C_1, C_2 and C_3 are the constants.

In the Ekman layer, K_m is constant, the wind stress decreases with height, and the vertical wind distribution is assumed to be specified by Ekman's solution. Let us represent the components of U and G as (u, v) and (u_g, v_g) respectively, and define the deviation of U from G as

$$W=(u-u_g)+i(v-v_g) \tag{4.4}$$

then the solution is

$$W=W_he^{-\beta(z-h)}\cdot e^{-i\beta(z-h)} \tag{4.5}$$

where W_h is the W at the height h, and

$$\beta=\sqrt{f/2K_m} \tag{4.6}$$

The inflow angle (ψ) and the friction velocity (U_*) are solved at the height h by connecting Equation (4.1) with Equation (4.5) with following boundary conditions,

$$\begin{aligned}&\vec{U}=0 && \text{at} \quad z=z_0\\ &\vec{U}=G && \text{at} \quad z=\infty\\ &\vec{U},\ \frac{\partial\vec{U}}{\partial z},\ \vec{\tau} && \text{are continuous through } z=h\end{aligned} \tag{4.7}$$

where $\vec{U}$, $\vec{G}$ and $\vec{\tau}$ are the vectors of wind, gradient wind and wind stress respectively. Using these results, Equation (4.1) can describe completely the distribution of wind in the surface layer. In our experiments, wind direction and wind speed at the height of 20 meters are used.

4.2 Numerical model of ocean wind waves

Numerical computation of the waves were performed by means of our model (ISOZAKI and UJI, 1973). The model is based on the radiative transfer equation, and contains five energy transfer processes. These are the linear and exponential wave growths with time, wave breaking, frictional dissipation and the effect of opposing winds. Expressions for each mechanism were developed from considerations of available theoretical and experimental results.

Some computational devices were developed for the computation of wave propagation which displays reasonable dispersion and angular spreading.

The basic equations of the model are given by

$$\left.\begin{aligned}
&\frac{\partial S}{\partial \mathrm{t}}=-\boldsymbol{C}_g\cdot\nabla S+(A+B\cdot S)\left\{1-\left(\frac{S}{S_\infty}\right)^2\right\}\cdot\Gamma(\theta), && S\leqq S_\infty,\ \theta<90^\circ\\
&\frac{\partial S}{\partial t}=-\boldsymbol{C}_g\cdot\nabla S-D\cdot f^4 S, && S>S_\infty,\ \theta<90^\circ\\
&\frac{\partial S}{\partial t}=-\boldsymbol{C}_g\cdot\nabla S-\{B\cdot\Gamma(\theta)+D\cdot f^4\}S, && \theta>90^\circ
\end{aligned}\right\} \qquad (4.8)$$

where θ is the angle between directions of wind and wave propagation, and $\Gamma(\theta)$ the angular distribution of the two-dimensional wave growth, S the two-dimensional energy spectrum, $\boldsymbol{C}_g$ the group velocity of the wave component, A and B the linear and exponential growth rates respectively, D the constant which represents the energy dissipation, and S_∞ the fully developed wave spectrum.

Now our knowledge about the two-dimensional wave growth is small, and $\Gamma(\theta)$ is replaced by the rule of $\cos^2\theta$. The rates of wave growth A and B are represented here by the results of INOUE (1967) for expedience. The constant of frictional dissipation D is so determined experimentally that the wave components shorter than 3 sec will die out within one hour if there is no energy supply from winds. Fully developed wave spectrum S_∞ is assumed here to have a functional form which was proposed by PIERSON and MOSKOWITZ (1964), that is

$$S_\infty(\omega)=\frac{\alpha g^2}{\omega^5}e^{-\beta(g/U\omega)^4} \qquad (4.9)$$

where $\alpha=0.83\times10^{-2}$ and $\beta=0.74$; ω is the angular frequency g the gravitational acceleration.

The solution is obtained directly by the integration of Equation (4.8) with respect to time using finite difference scheme. A wave spectrum consists of 21 frequency components from 0.04Hz to 0.25Hz with 0.01Hz-band width. Each frequency com-

ponent is divided into 16 directional components according to its propagation direction. The frequency components higher than 0.25Hz are assumed to maintain always the limiting energy level corresponding to the local winds.

4.3 Computation of waves in a wide area (Test-1)

Computations of waves were performed for the period of eight days from 3^h, Aug. 26 to 15^h, Sept. 2, 1974. At the first step, computation is made over a wide area with rough meshes, and rough aspects of the waves caused by Typhoon 7416 are obtained (Test-1). Next, the waves over Sagami Bay are computed with fine meshes using the results obtained in Test-1 as a boundary condition (Test-2).

Fig. 9 shows the computation domain and grid distribution used in Test-1. Grid interval of 170 km and a time step of 6 hours are adopted. As basic data, sea level atmospheric pressure, surface air temperature and sea surface temperture are read six hourly from weather maps prepared by the Japan Meteorological Agency. Next, marine surface wind at 20 meter-height are calculated on each grid point using these meteorological information. Then, wave spectra and wave heights are obtained by use of the numerical model based on the estimated marine surface winds.

Fig. 10 shows an estimated wind distribution at 9^h, Aug. 30, 1974, when the typhoon was about 850 km south off the Boso Peninsula. In this figure are seen a gale wind area more than 40 m/s in the southeastern sector of the typhoon and a rather weak storm in the western sector, in agreement with the well-known combination of the dangerous and navigable semicircles. But the wind velocity of

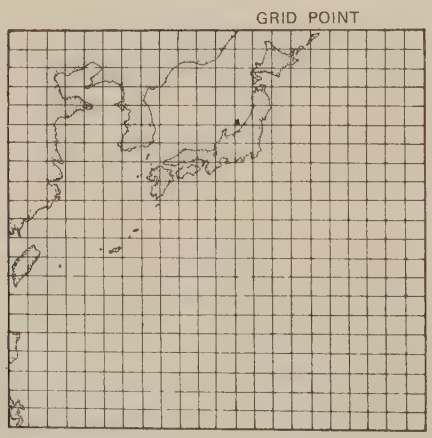

Fig. 9. Grid used to specify wind and wave fields in Test-1. (mesh size: 170 km)

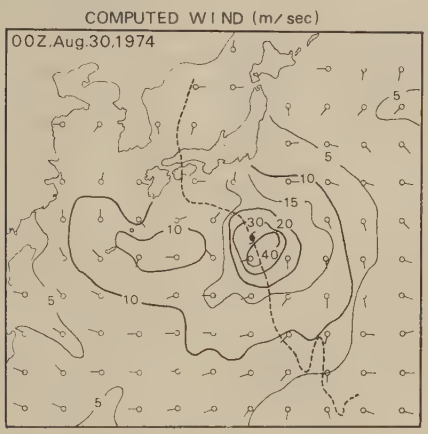

Fig. 10. Distribution of predicted surface winds at 9h, Aug, 1974.

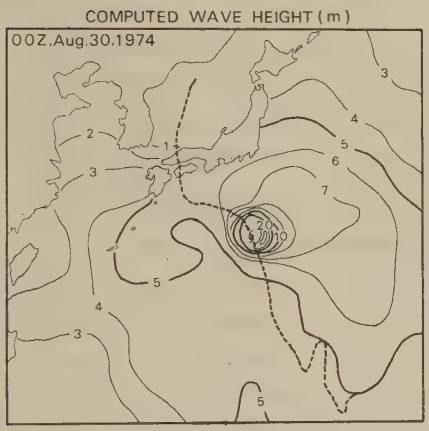

Fig. 11. Distribution of predicted wave heighi at 9h, Aug. 30, 1974.

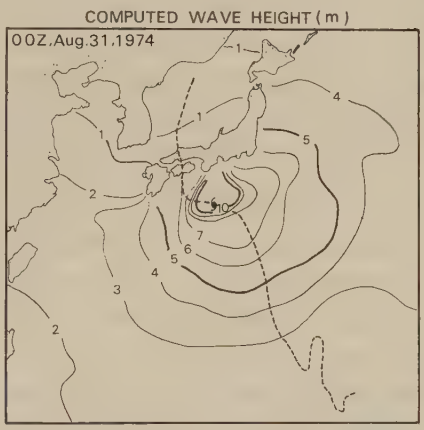

Fig. 12. Distribution of predicted wave height at 9h, Aug. 31, 1974.

more the 40 m/s is too large considering that the value of wind velocity means the six hours average in our experiments. Overestimation of wind velocity in a typhoon area results in overdeveloped wave situation especially for low-frequency wave components in our computation.

Fig. 11 and 12 show the distributions of computed wave height at 9h, Aug. 30 and 9h, aug. 31, 1974. In Fig. 11, wave height in the eastern semicircle of the typhoon area is higher than those in the western semicircle, and the maximum wave height of more than 20 m is seen about 150 km east-southeast from the typhoon center. The distribution of wave height is similar to that in usual typhoon area,

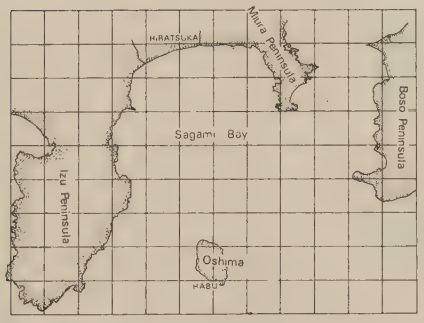

Fig. 13. Grid used to specify wind and wave fields in Test-2. (mesh size: 10 km)

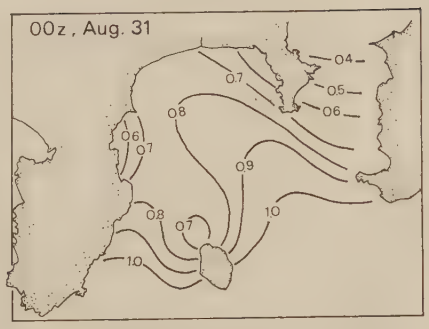

Fig. 1. Distribution of predicted relative wave height at 9h, Aug. 1974.

but the height of 20 meters seem to be too high. The wave height distribution in Fig. 12 has similar characteristics to the distribution in Fig. 11, and the maximum wave height, about 10 meters, is reasonable. Mesh size of 170 km used here is not adequate to represent winds and waves in a tyhoon area precisely because of large variability of local meteorological conditions near a typhoon center. Nevertheless, the distributions of winds and waves obtained in this experiments were reasonable except a few over-estimation of winds and waves near the typhoon center.

4.4. Computation of waves over Sagami Bay (Test-2)

Computations of the waves over Sagami Bay were made with fine meshes to represent local characterics of the waves. The period of computaton is 8 days from 3h, Aug. 26 to 15h, Sept. 2, 1974, as same as Test-1. Fig. 13 shows the computation domain and the grid distribution used to specify wind and wave fields in Test-2. Grid size is 10 km and time step is one hour. Wind data are prepared by interpolation with respect to time and space between the winds produced in Test-1 and those observed on the coast of Hiratsuka. The conditions on the outer boundary over the ocean are specified by interpolation with respect to time and space between the wave spectral values estimated on the two grid points of rough meshes in Test-1.

Fig. 14 shows a distribution of estimated relative wave height which is defined as the ratio of local wave height to the wave height at Habu-harbor. In general, waves in Sagami Bay is smaller than the waves outside the bay. A high wave area is seen on the central part of the bay stretching to north-northwest from the mouth of the bay. Wave height on the Uraga Straits is less than a half of the heights outside the bay by the effect of sheltering caused by the Boso Peninsula. It is seen

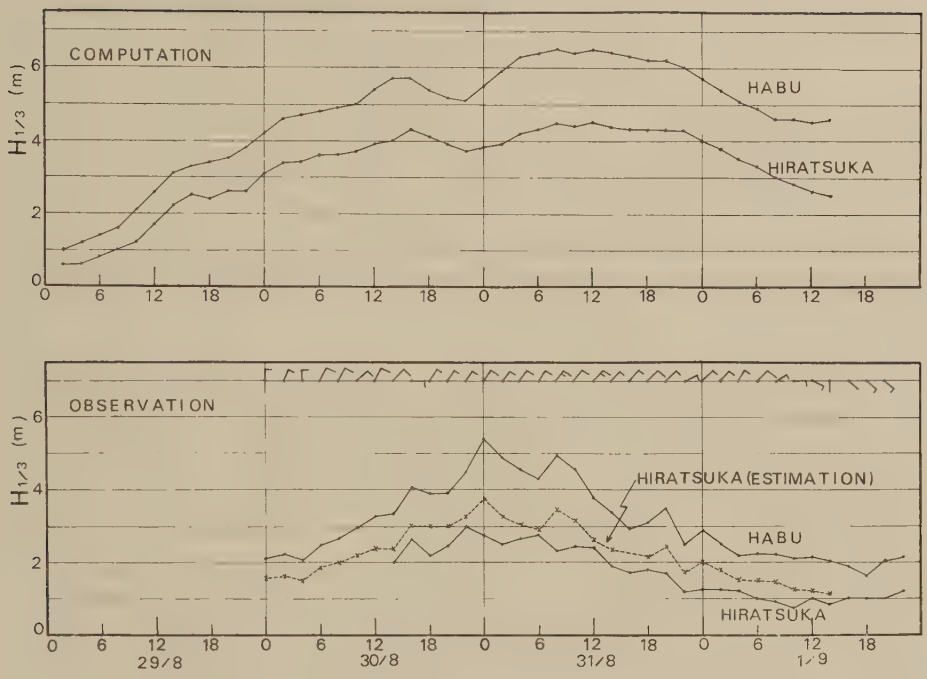

Fig. 15. Time variation of predicted and observed weve heights off Habu-harbor and Hiratsuka from Aug. 20 to Sept. 1, 1974.

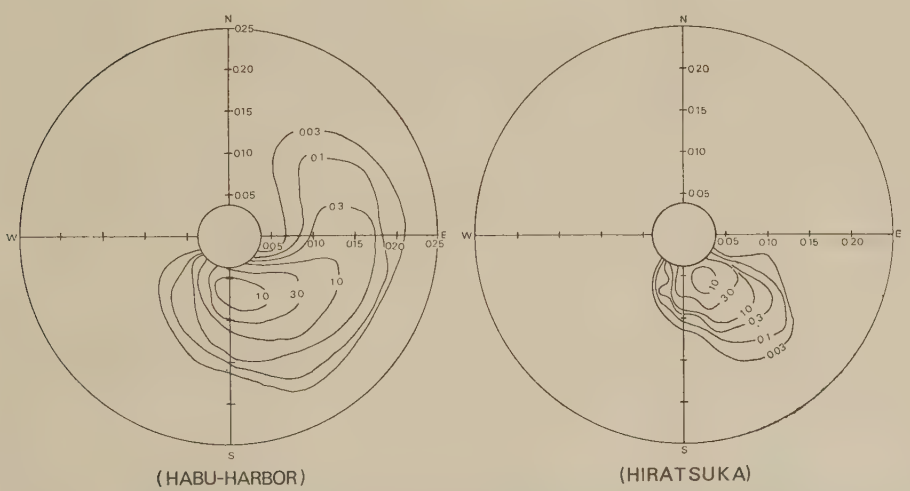

Fig. 16. Predicted two-dimentional wave spectra off Habu-harbor and Hiratsuka at 9h, Aug. 31, 1974.

that the sheltering effect caused by Oshima Island reduces the wave height remarkably on the sea area extending to north-northwest from the island. The relative wave height off the coast of Hirastuka is about 0.7, that is, the wave height off the coast of Hiratsuka is abut 30% less than the height off Habu-harbor.

Fig. 15 shows the time variation of wave height at Hiratsuka and Habu-harbor. The upper part of the figure represents the wave heights obtained by the computation in Test-2, and two full curves in the lower part of the figure represent the observed variation of wave height. As has been discussed previously, the computed wave heights are larger than the observations reflecting the overestimated wind speed near the typhoon center. But the difference of wave heights between Hiratsuka and Habu-harbor is clearly reproduced in the prediction. That is, the predicted wave heignt at Hiratsuka is about 30% less than the height at Habu-harbor. The reduction of the predicted wave height may be caused in our numerical model by frictional dissipation, decay due to opposing winds and sheltering effects of peninsula and island. But the first two effects can be neglected in the present experment, because the waves in consideration are swell which have large parts of its energy in the lower frequency wave components, traveling distance from Oshima Island to the coast of Hiratsuka is about 60 km, and breeze or moderate winds are prevailing over the bay through out the present computation period.

If the reduction factor of wave height obtained above is applied to the wave height observed at Habu-harbor, we can find the wave height off the coast of Hiratsuka which have been reduced by the sheltering effect of the Boso, Miura and Izu Peninsulas. Variation of thus estimated wave height is shown by a broken line in the lower part of Fig. 15. The estimated wave height is somewhat larger than the one observed at Hiratsuka. The application of wave height reductions due to the shoaling and the refraction in a shallow water region to the estimated wave height may yield finally estimated wave height witch agrees reasonably well with the observations taken at the Oceanographic Observation Tower, Hiratsuka.

Fig. 16 shows two-dimentional wave spectra off Habu-harbor and Hiratsuka at 9^h, Aug. 31, 1974 predicted in the computation of Test-2. In this figure, distances from the center of the circle to the radial direction represents the frequency of wave components, the directon of radius is the orientation from which each wave componet incidents, and contours represent energy density in units [m^2 sec]. It is seen in the spectrum at Habu-harbor that a large part of wave energy comes from south-southeast associated with minor wave energy coming from rather widely spread directions from northeast to southwest. On the other hand, the spectrum at Hiratsuka

has narrow directional spreading of wave energy showing sharp concentration in the wave componets coming from southeast and south-southeast.

5. Conclusion

Remarkable swell is observed on the coasts of the Kanto and Tokai Districts when Typhoon 7416 passed on the sea several hundred kilometers south off the coasts. The report explained the characteristics of two sets of the swell data taken at the Oceanographic Observation Tower, Hiratsuka and on the sea bottom off Habu-harbor, Oshima Island.

Breeze or moderate northeasterly winds prevailed over Sagami Bay during the period from Aug. 30 to Sept. 1 when remarkable swell observed at Hiratsuka and Habu-harbor. Accordingly the swell seems not to be followed by notable local wind waves nor be suppressed by the effect of opposing winds. Nevertheless, the wave height observed at Hiratsuka is about 40% lower than the one observed at Habu-harbor in average.

The difference of wave heights between the two stations are reproduced reasonably well through the numerical experiments. It is concluded that the wave height taken at Hiratsuka is reduced from the height at Habu-harbor about 30% by the effect of the sheltering caused by the peninsulas and about 10% by the effects of the shoaling and the refraction near the Tower.

It is surprising that the swell caused by Typhoon 7416 reached the coast of Hiratsuka from the bay mouth suffering the wave height reduction of about 30%, in spite of travel direction of the swell which incidented in Sagami Bay normally.

Finally, we emphasize that the results of wave observation near coast may be used effectively to supplement the lack of wave data if careful procedures are made to correct the distortion due to the sheltering, shoaling, refraction, diffrection, refrection and several energy dissipation processes.

Acknowledgments

The authors sincerely wish to thank Dr. N. Iwata and all members of the Institute of Coastal Oceanography, National Research Center, Hiratsuka who offered every facility to us on the wave observations at the Oceanographic Obesrvation Tower. Mr. T. Takahashi is acknowleged for his help in preparing wave data taken at Habu-harbor, Oshima Island.

Dr. T. Nannichi is also acknowledged for his advice and careful reading of this manuscript.

References

ARTHER, R.S., W.H. MUNK, and J.D. ISSACS (1952): The direct construction of wave rays. Trans. Am. Geophys. Un. **33**, 855–865.

BARNETT, T.P. (1968): On the generation, dissipation, and prediction of ocean wind waves. J. Geophys. Res., **73**, 513–529.

BARNETT, T.P., C.H. HOLLAND, Jr. and P. YAGER (1969): A general technique for wind wave prediction, with application to the South China Sea. Final Report, Contract N62306–68–0285, U.S. Naval Oceanographic Office, 31p.

BLACKADAR, A.K. (1965): A simplified two-layer model of the baroclinic neutral atmospheric boundary layer. Air Force Cambridge Res. Lab. Report 65–531, 49–65.

CARDONE, V.J. (1969): Specification of the wind distribution in the marine boundary layer for wave forecasting. New York Univ. School of Engineering and Science, Report GSL–TR–69–1, 131p.

DEXTER, P.E. (1974): Tests of some programmed numerical wave forecast models. J. Phy. Oceanogr., **4**, 635–644.

EWING, J.A. (1971): A numerical wave prediction method for the North Atlantic Ocean. Deut. Hydrogr. Zeit., **24**, 241–261.

GELCI, R.H. and E. DEVILLAZ (1970): La calcul numérique de l'etat de la mer. Houille Blanche, **25**, 117–131.

INOUE, T. (1967): On the growth of the spectrum of a wind generated sea according to a modified Miles-Phillips mechanism and its application to wave forecasting. Geophy. Sci. Lab. Report No. TR67–5, New York Univ. 74p.

ISOZAKI, I. and T. UJI (1973): Numerical prediction of ocean wind waves. Pap. Meteorol. Geophy., **24**, 207–231.

ISOZAKI, and T. UJI (1974):Numerical model of marine surface wind and its application to the prediction of ocean wind waves. Pap. Meteorol., Geophys. **25**, 197–231.

PIERSON, W.J., L.J. TICK and L. BAER, (1966): Computer based procedures for preparing global wave forecasts and wind analysis capable of using wave data obtained from a space-craft. 6th Symposium on Naval Hydrodynamics, **2**, 1–42.

WILSON, W.S. (1966): A method for calculating and plotting surface wave rays. Tech. Memo. No. 17, U.S. Army Coastal Engineering Research Center. 57p.

台風7416号によって起こった相模湾上の波

磯崎一郎・宇治豪

（気象研究所）

瀬戸力・海悦明

（東海大学海洋学部）

相模湾奥の平塚海岸（防災科学技術センター平塚支所の海洋観測塔）および湾口の大島波浮港沖で観測された台風7416号による波の性質についての解析結果を述べる。気象条件を考え合せるとこの時の波浪はほとんどうねりであると考えてよい。

両地点での波高の時間変化の傾向は非常によく似ているにもかかわらず，平塚の波高は波浮港の値にくらべて平均的に40%も低かった。この相違の原因を解明するためには数値実験を行なったが，その結果によるとこのうねりは湾口から平塚海岸に到達するまでに房総半島と伊豆半島の遮蔽効果によって約30%の波高減少を起こす。さらに，平塚の海洋観測塔近傍での浅水効果と屈折効果によって約10%の波高減少が起こり得る。これらの値は観測された平塚と波浮港の波高の相違と合理的に一致する。

結局，海岸近傍での波浪観測データでも，遮蔽・浅水・屈折・回折・反射などの諸効果について注意深い補正を行なえば外洋波浪の状態を推測するために効果的に用い得ることが確かめられた。

The Oceanographical Magazine
Vol. 27, Nos. 1-2, pp. 25 to 36, March 1976

Direct measurement of deep sea current by Richardson-type current meters in the western-north Pacific

Koichi NAGASAKA

Japan Meteorological Agency

(Received November 22, 1975)

Abstract: Deep sea current measurements were carried out at three stations in the western north Pacific east of the Izu-Ogasawara Trench by moored Richardson-type current meters. The durations of observations were 86, 238 and 70 hours, respectively and the height of the current meter above the bottom was 110 meters at each station. The mean current speed ranged from 1.8 to 5.4 cm/s with the mean current directions mostly from southerly to westerly and the maximum speed was more than 10 cm/s. The semi-diurnal and the diurnal periods were dominant at every station. The Power spectra agreed with the $-5/3$ law for the high frequencies up to the diurnal period.

Introduction

Although the determination of deep sea current is very important and useful to reveal the general circulation of the ocean and also the practical purposes such as marine engineering, still our knowledge of deep water motion is extremely limited compared with that of sea surface and subsurface. Especially the direct measurement of deep sea current has been slowly and sporadically carried out because of the difficulty in instrumentation and operation. Among the various methods the technique of moored Richardson-type current meter seems to be a most effective and attractive one to obtain long-period, continuous current records in deep sea layers.

Current measurements right above the ocean floor by moored Richardson-type current meters were made at three stations in the western-north Pacific. Geographic positions of the station of mooring are shown in Fig. 1. Every mooring had a current meter at the height of 110 meters above the bottom and at the station C an additional current meter was equipped about 50 meters above the bottom.

Recording of current was successfully achieved for the periods of 86, 238 and 70 hours, respectively. These measurements were intended not only for study-

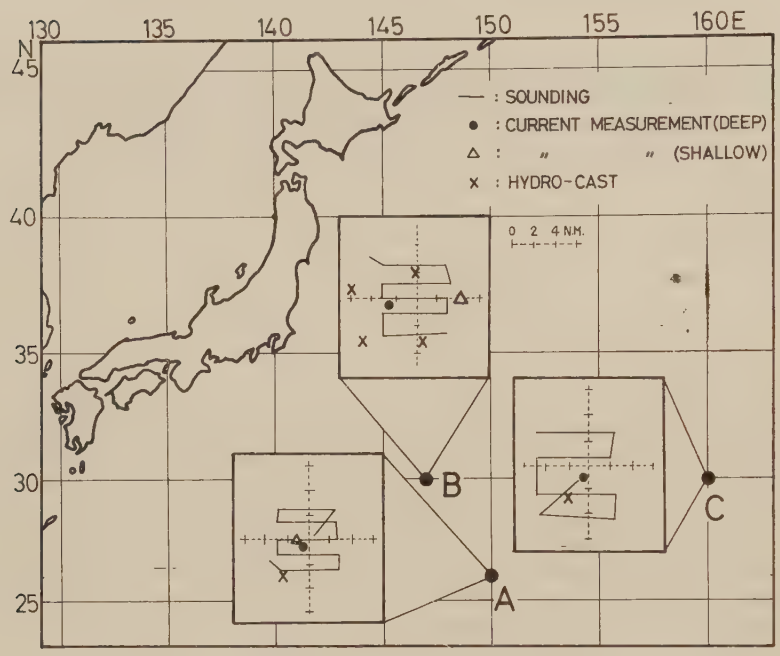

Fig. 1. The positions of the three moorings.

ing the water motion near the sea floor but also for testing the mooring technique including the anchor release system. Such mooring technique had not been established in our working group.

In the present breif paper the author would like to report briefly the method of the mooring and the preliminary results of the measurements. Further discussion on the obtained record will be left for a future paper.

Method of measuring deep sea current

The moorings of current meter were made at 25° 59′ N, 149° 59′ N (St. A) from November 14 through 18 in 1973, at 29° 59′ N, 146° 55′ E (St. B) from December 10 through 20 in 1974 and at 29° 58′ N, 159° 59′ E (St. C) from March 19 through 22 in 1975, respectively. Those stations were located east of the Izu-Ogasawara Trench of the western-north Pacific. The water depth of each station was 5885, 6200, and 5675 meters, respectively and the bottom topography in the vicinity of the mooring was sounded by R/V Ryofu Maru prior to launching the current meter.

The method of mooring of current meters is schematically shown in Fig. 2.

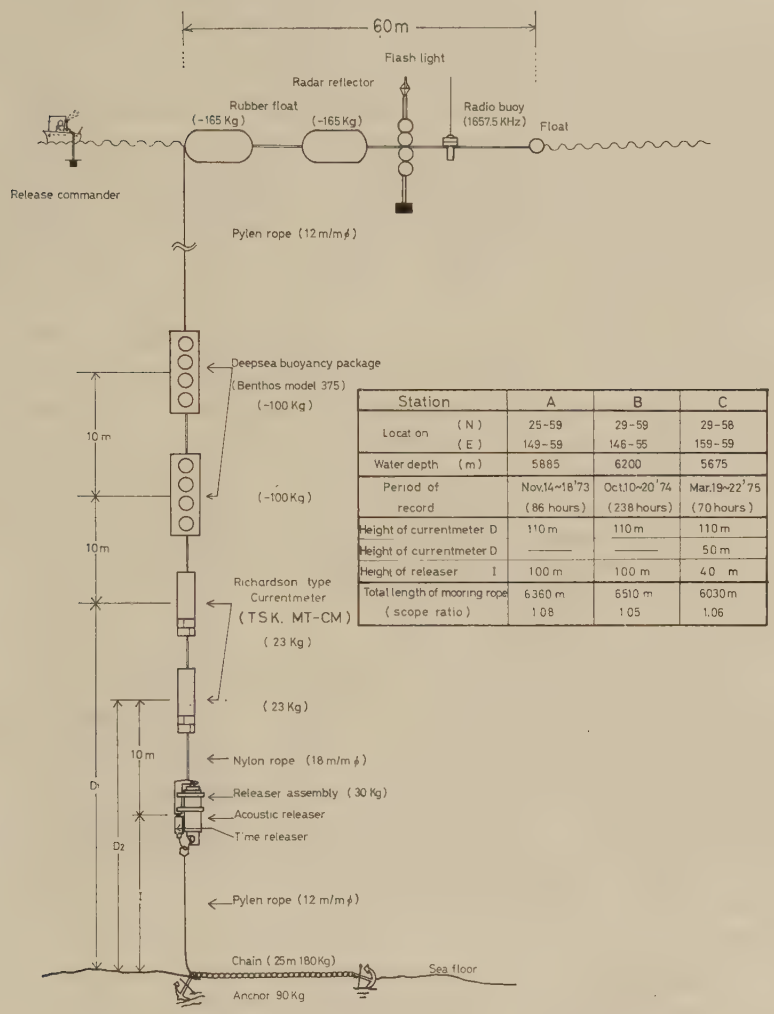

Station	A	B	C
Locat on (N)	25-59	29-59	29-58
(E)	149-59	146-55	159-59
Water depth (m)	5885	6200	5675
Period of record	Nov.14~18'73 (86 hours)	Oct.10~20'74 (238 hours)	Mar.19~22'75 (70 hours)
Height of currentmeter D	110 m	110 m	110 m
Height of currentmeter D	———	———	50 m
Height of releaser I	100 m	100 m	40 m
Total length of mooring rope	6360 m	6510 m	6030 m
(scope ratio)	1.08	1.05	1.06

Fig. 2. The mooring of deep sea current measurement.

The current meter used in the present observations is an MT-CM III (Magnetic Tape recording type Current Meter model III) manufactured by the Tsurumi-Seiki Co. and the mechanism of which is essentially the same as that of the Savonious type current meter invented by Richardson (Richardson et al., 1963). Each current meter was set to record the current for twenty seconds at five minutes intervals.

The mooring system consists of two 90 kg anchors, a 180 kg chain along the sea floor, anchor releases, a current meter, submerged buoys, a mooring rope

and surface buoys. Much effort was made to eliminate the effect of the motion of current meter itself on the record. In order to keep the current meter steady two packages of submersible buoys (the Benthos Co., Deep Sea Buoyancy Package model 375) with a buoyancy of 100 kg were attached just above the current meter. The anchor release was equipped between the current meter and anchor to release the latter for recovering the instruments easily and safely after the observation. Although an acoustic commanding type release (the Inter Ocean Co. model 100-DR) and a timed release (the Kaihatsu Kogyo Co., model KT-1) were equipped in parallel to make sure, the acoustic release perfectly responsed to the command transmitted at a distance of more than five miles from the surface buoys. Surface buoys were supplementally used to locate the surfaced current meters because neither a submersible light nor a submersible radio beacon was available. The surface buoys were consisted of two rubber floats of which buoyancy was 330 kg in total, a radio beacon, a flash light and radar reflector. A pylen cross rope of 12 mm in diameter which was slightly longer than the depth of water linked the submerged buoy and the surface buoy. The total length of the mooring line was 6360 at St. A, 6510 at St. B and 6030 meters at St. C and the scope ratio was 1.08, 1.05 and 1.06, respectively.

The technique used in Japan Meteorological Agency for launching of deep sea mooring system is usually "surface buoy first, anchor last" method. The sequence of operation is; launching surface buoys; paying out the entire mooring line length while underway and finally launching and letting the instrumentation, chain and anchors freely sink. In the present mooring the chain and the anchors reached the bottom within an hour after the launching. The recovering of the instruments was easily achieved by pulling the mooring line after the chain and the anchors were released.

Results of measurements

The record on the magnetic tape was automatically read out by the processor specially designed for this current meter. During the processing not only the correction of current direction for the local magnetic variation but also the correction of current speed for the inclination of the current meter was made. In order to obtain the corrected speed the value of observed speed was divided by the cosine of the tilt angle of the instrument. The inclination of the device was less than ten degrees except at St. B, where it was as much as fifteen degrees during almost entire period of the observation. This suggests that the submerged buoys with a

buoyancy of 200 kg was effective to keep the instrument in attitude as expected.

The current speed, the current direction, the inclination of the current meter and eastward and northward components of the velocity were measured in this study. Since current speeds below the threshold level of the current meter (about 1.8 cm/s) were not reliable, such portions of the record were estimated by extrapolating time-velocity relations obtained for current speed higher than 1.8 cm/s. The current speed and the current direction were read from these smoothed curves for every thirty minutes. All the following statistical study was done by using those read-out values.

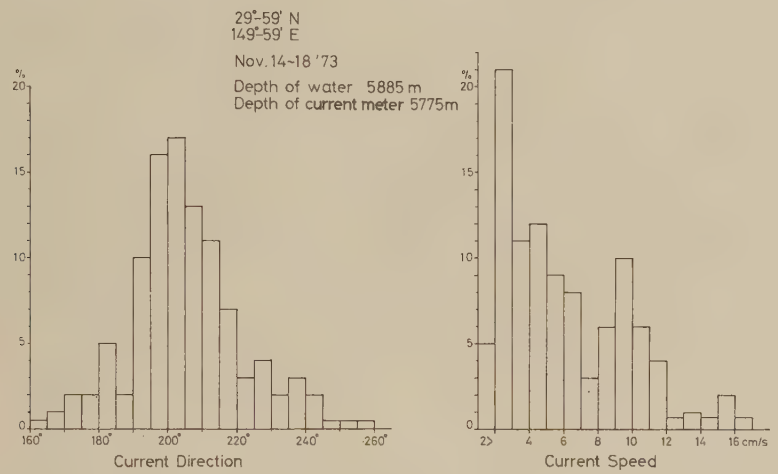

Fig. 3. The histgrams of the current speed and the current direction at St. A.

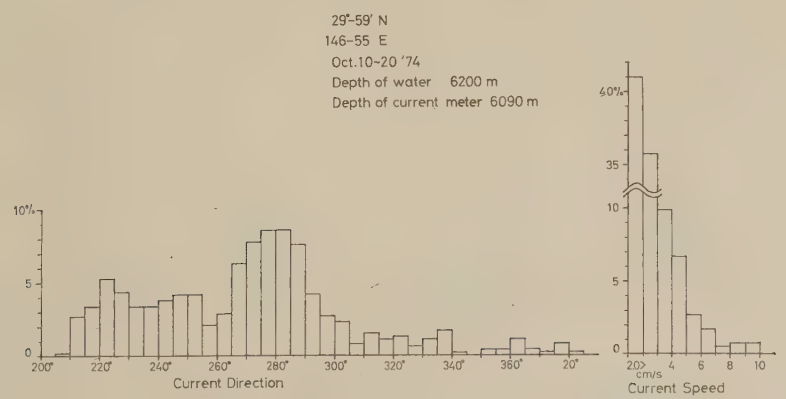

Fig. 4. The histgrams of the current speed and the current direction at St. B.

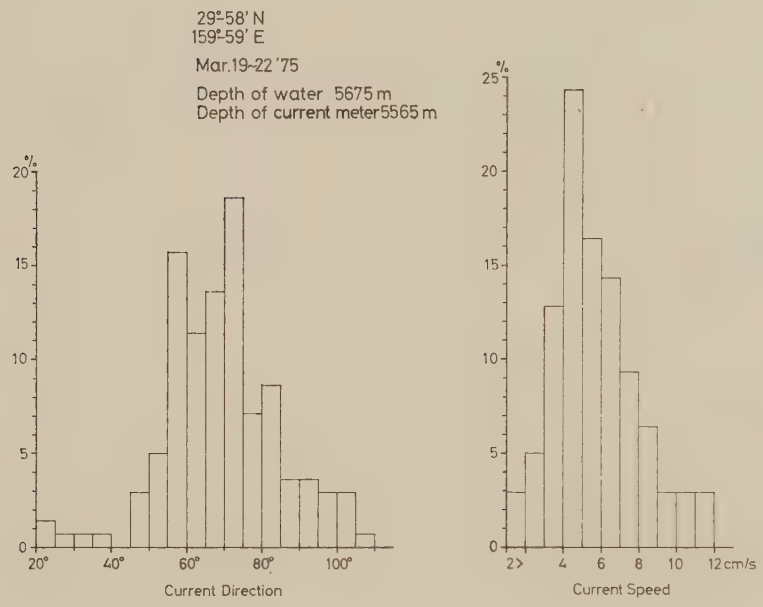

Fig. 5. The histgrams of the current speed and the current direction of the upper layer at St. C.

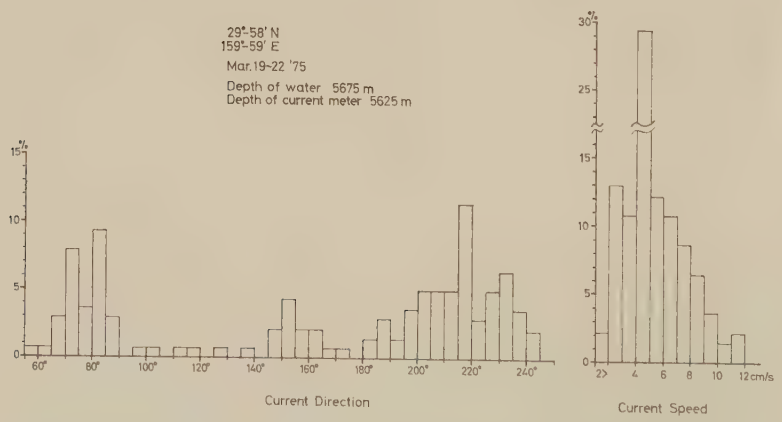

Fig. 6. The histgrams of the current speed and the surrent direction of lower layer at St. C.

The maximum speed, the vector averaged current speed and direction are summarized as follows.

Station	Max. Speed	Mean speed	Mean direction
St. A	16.4 cm/s	4.8 cm/s	209° T
St. B	10.5	1.8	272
St. C (upper)	12.2	5.4	70
St. C (lower)	11.9	2.7	171

Those mean speeds obtained are almost of the same order as that observed in the depths ranged from 2000 to 5000 meters in the western-north Pacific reported by several authors (Takenouti et al., 1962, Yasui and Nan'niti, 1962, Nan'niti et al., 19664, and Nan'niti et al., 1965).

Fig. 3 to 6 show the histgrams of the current direction and the current speed of each measurement. At St. A the current direction ranged from 160° T to 260° T, and directions around 200° T were most frequent. The histgram of the speed had three peaks around 2.5, 4.5 and 9.5 cm/s. At St. B the range of the current direction was wider than that of St. A, and two peaks, around 225° T and 280° T, were recognized. The speeds below 2.0 cm/s were most frequent. At St. C the

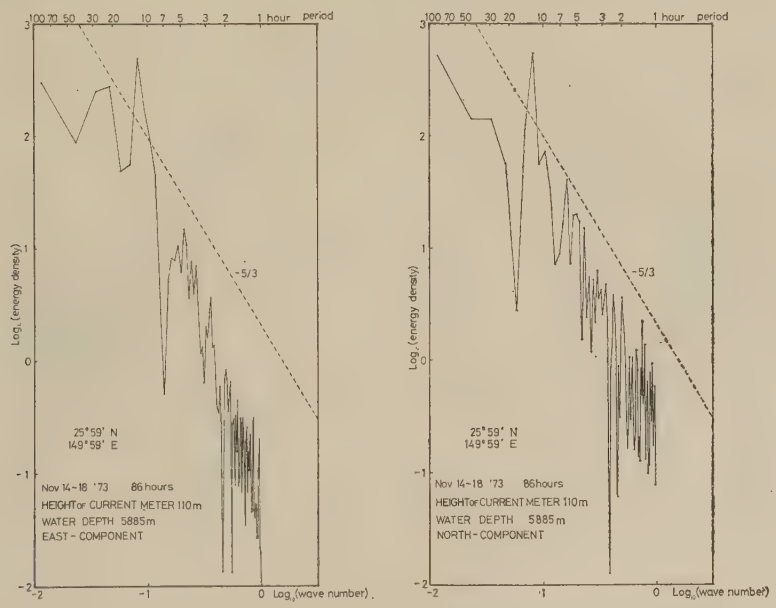
100 70 50 30 20 10 7 5 3 2 1 hour period
-5/3
25°59' N
149°59' E
Nov 14~18 '73 86 hours
HEIGHT of CURRENT METER 110 m
WATER DEPTH 5885 m
EAST - COMPONENT
NORTH - COMPONENT
Log10 (energy density)
Log10 (wave number)

Fig. 7. Power spectra of the eastward and northward components at St. A.

upper current meter (110 meters above the bottom) recorded current directions ranging from 20° T to 120° T with peaks around 75° T, 55° T and 85° T, and the current speeds between 4 and 5 cm/s were most dominant. On the other hand the record of the lower current meter showed a wide range in direction, from 55° T to 245° T. But the frequency distribution of the current speed was very similar to that measured by the upper current meter. The fluctuations of the speed in the upper layer and lower layer occurred simultaneously but the fluctuations of the current direction occurred independently especially in the latter half of the observation period. It is difficult to find the cause of this difference even if the effect of turbulence in bottom layer is taken into consideration.

The power spectrum of each component of the velocity is shown in Figs. 7 to

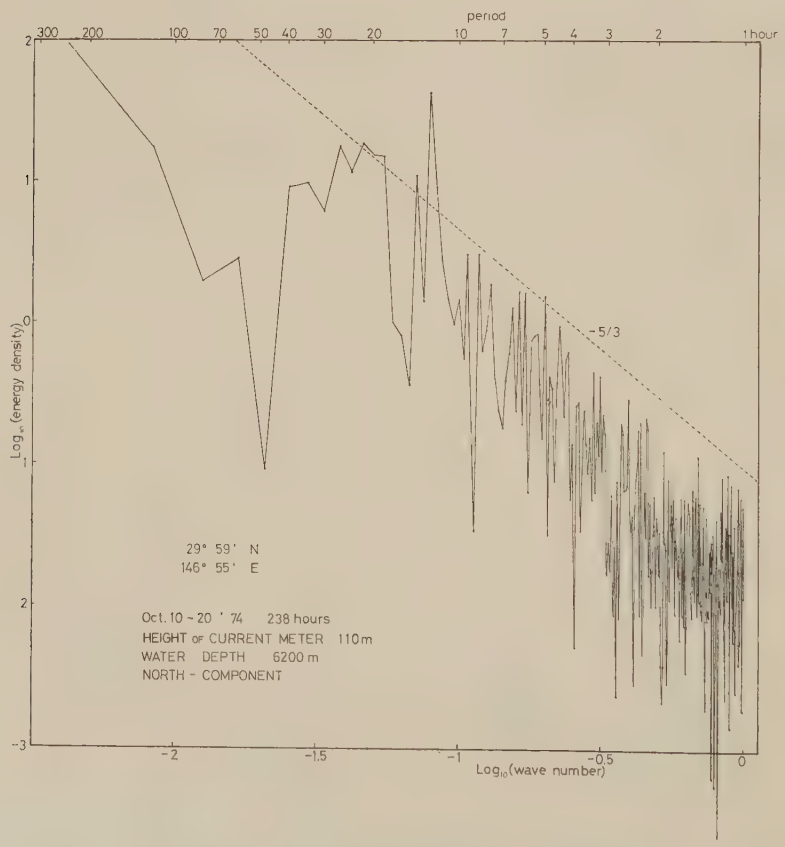

Fig. 8-a. Power spectrum of the northward components at St. A.

10. Although the periods of the measurements were insufficient for precise analyses, the diurnal and semidiurnal fluctuations were apparent at each station. The periods of the local inertia motion at the present stations are approximately equal to 24 lunar hours, so it is almost impossible to separate the diurnal motion of tide from the local inertia motion by such short-term observations. Some long-term fluctuations with periods more than a week are suspected to exist from the record at St. A. To clarify these problems longer-term observations are desirable in future. The spectra at each station agreed with the −5/3 law for the frequencies up to the diurnal period.

Four hydrocasts down to the bottom were carried out around St. B. From the hydrographic data the current profile referred to 6000 db was calculated as shown

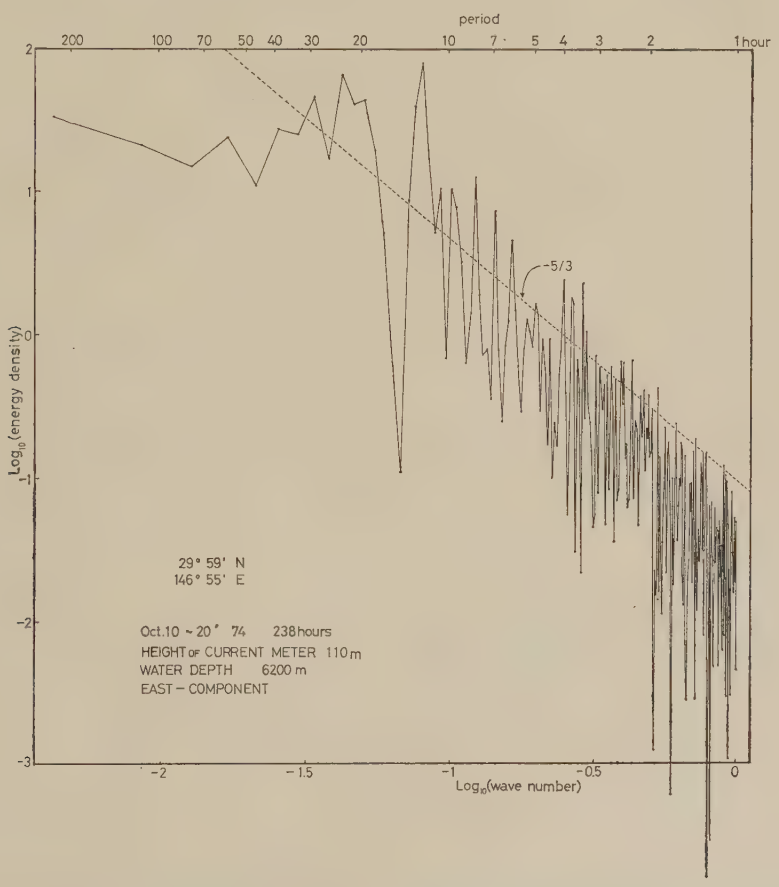

Fig. 8-b. Power spectrum of the eastward components at St A.

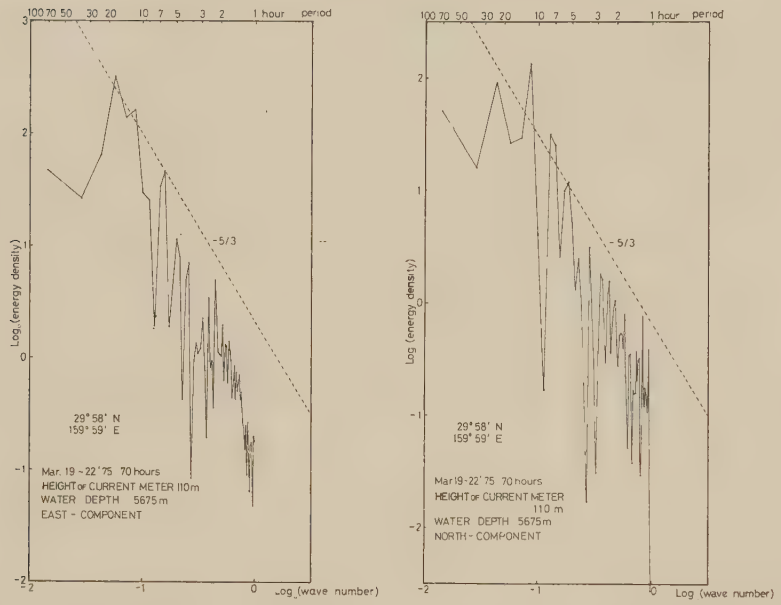
100 70 50 30 20 10 7 5 3 2 1 hour period
-5/3
29°58' N
159°59' E
Mar. 19 - 22'75 70 hours
HEIGHT of CURRENT METER 110m
WATER DEPTH 5675m
EAST - COMPONENT
Log (energy density)
Log (wave number)
Mar19-22'75 70 hours
HEIGHT of CURRENT METER 110 m
WATER DEPTH 5675m
NORTH - COMPONENT

Fig. 9. Power spectra of the eastward and northward components of the upper layer at St. C.

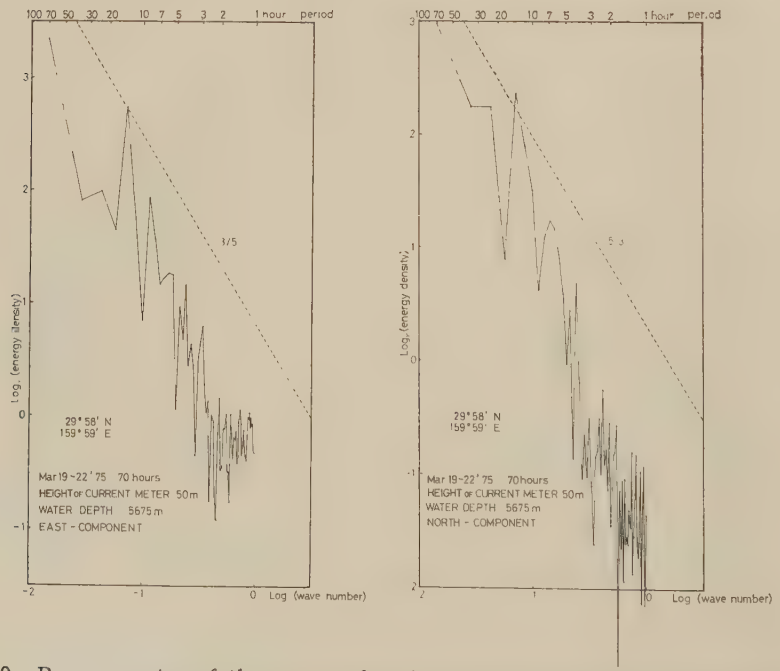

Fig. 10. Power spectra of the eastward and northward components of the lower layer at St. C.

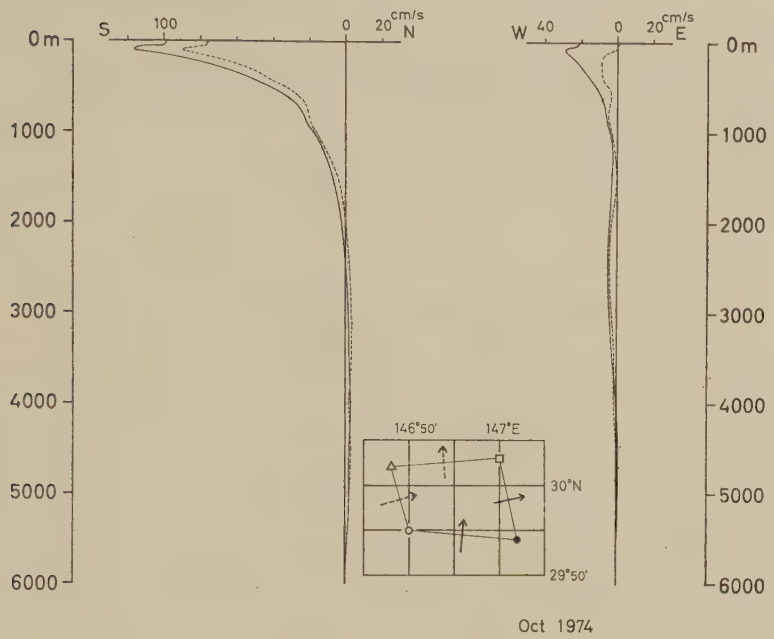

Fig. 11. Geostrophic current at St. B.

in Fig. 11. The highest dominant current appeared at the depth of 50 meters. In the layer, the dinamically computed speed is more than 100 cm/s and the composed direction is 220° T.

Deep sea current determinations near the ocean floor are very few in the Pacific. More observations and longer-term measurements have to be carried out to study the water motion near the bottom.

Acknowledgments

The author would like to express his heartfelt thanks for the cooperation of corabolators in the observation, and the officers and crew on board R/V Ryofu Maru.

References

RICHARDSON, W.S., STIMSON and C.H. WILKINS, 1963 Current measurement from moored buoys. Deep-Sea Res., 10: 369–388.

TAKENTUTI, Y., T. NAN'NITI and M. YASUI, 1962 The deep-current in the sea east of Japan. Oceanogr. Magaz., 13 (2): 89–102.

YASUI, M. and T. NAN'NITI, 1962 Deep-sea current measurement during the JEDS-4. Oceanogr. Magaz., 13 (2): 133-136.
NAN'NITI., T., H. AKAMATSU, T. NAKI and K. FUJII, 1964 An observation of a deep current in the Southern East Sea of Tori-shima. Oceanogr. Magaz., 15 (2): 113-122.
NAN'NITI., T., H. AKAMATSU and T. NAKAI, 1964 A further observation of a deep current in the East-North-East Sea of Torishima. Oceanogr. Magaz., 16 (1-2): 11-19.
NAN'NITI, T., H. AKAMATSU and T. NAKAI, 1965 A deep current measurement in the Honshu Nankai, the sea south of Honshu, Japan. Oceanogr. Magaz., 17 (1-2): 77-86.

北大平洋における係留されたリチャードソン型流速計による深層流の測定

長　坂　昂　一

（気象庁海洋気象部）

北西太平洋の25°59′N, 149°56′E（A, 水深 5885m), 29°59′N146°55E (B, 6200m) 29°59′E (C, 5675 m）の3点において海底直上110m（一部では50mも）の海流をブイに保留されたリチャードソン流速計により計測した。計測期間はそれぞれ86, 238, 70時間で，次のような流れが測定された。

測点	最大流速	平均流速	平均流向
A	16.4m	4.8cm/s	209°T
B	10.5	1.8	272
C（海底直上 50m）	12.2	5.4	70
C（海底直上 50m）	11.9	2.7	171

測得流には日周期及び半日周期の変動が卓越していた。又，A点ではこの他に1週間以上の周期と思われる長周期変動が見られたが今回程度の測定期間では，はっきりしなかった。各測点での慣性流周期はほぼ1日であるため，日周期の変動が潮汐流によるののか慣性流によるものかは同様に今回程度の測定期間では判定できなかった。

各流速成分のパワー・スペクトラムの内で日周期未満の短周期変動については，コロモグロフの−5/3乗則に良く一致した。

The Oceanographical Magazine
Vol. 27, Mos, 1-2, pp. 37 to 41, March 1976

A Preliminary Report of Magnetic Surveys in GDP
Geomagnetic Anomaly Lineations in the Area Southwest of Shatzky Rise

Nobuhiro ISEZAKI

Meteorogical College

(Received December 22, 1975)

Abstract: In the Northwest pacific basin, the strike of anomaly lineations of geomagnetic total itensity is N 65° E. By recent magnetic surveys in a part of the Japanese Geodynamics Pɹojet program, another strike of anomaly lineations, N 50° E, is confirmed in the area south of 32°N latitude, between Bonin Trench and Shatzky Rise. The boundary of two areas seems to correspond to the bathymetric features which appear to cross over Shatzky Rise like some kind of a fault, but another tectonic mechanism also be involved, which resulted in the different strikes of magnetic anomaly lineations on both sides of the boundary.

1. Introduction

HAYES and PITMAN (1970) suggested a magnetic bight in the Northwest Pacific Basin and LARSON and CHASE (1972) presented plate tectonics in terms of of triple junction ridges in the North Pacific Ocean. HILDE *et al.* (1975) compiled the existing magnetic data presented detail distribution of anomaly lineations and identified their ages. All these authors supposed a magnetic bight, however, its clear feature has not been figured out because of sparse distribution of magnetic data, especially around Shatzky Rise.

Since 1972, magnetic surveys nave been carried out in the Japanese Geodynamics Project (GDP) program in the area concerned to get more confident lineations on the west side of the magnetic bight. This paper is a preliminary report of these magnetic surveys and complilation together with available American data.

2. Data Sources

Fig. 1 shows ship tracks along which magnetic hata are available. As part of the Japanese GDP program, we made magnetic surveys by R/V Ryofu Maru of the Japan Metorological Agency (1972) and R/V Tokaidaigaku Maru II of the University of Tokai (1972). The other Japanese data were by R/V Hakuho Maru of the

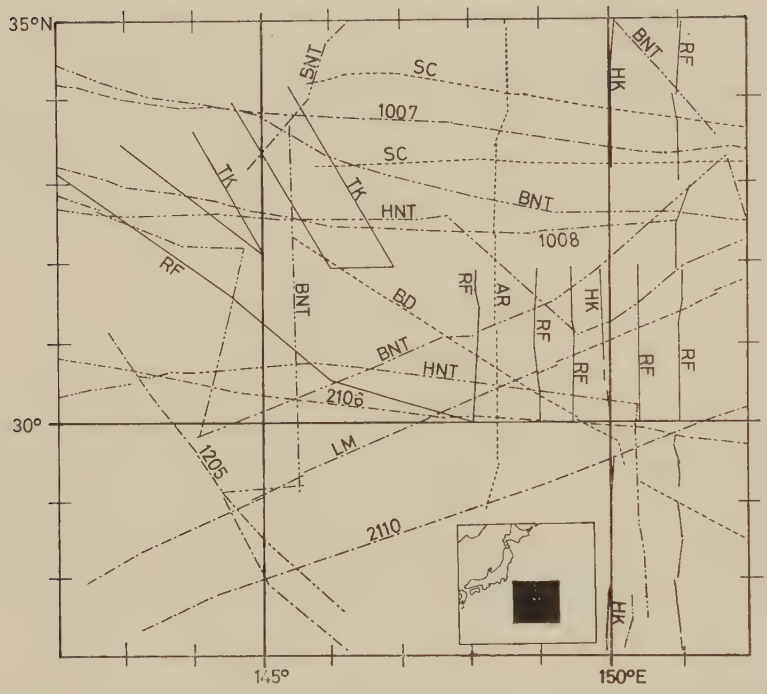

Fig. 1. Ships' track on which magnetic data ate available. —— Japanese tracks (RF, TK, HK), ---- Scripps tracks (AR, BD, SC), -·-·- Lamont tracks (numeric number, LM), -···- NAVOCEANO tracks (BNT, HNT),

University of Tokyo (KH-69, 1969).

American data are of the Scripps Institution of Oceanograpy of the University of California by R/V Argo (ZETES-4, 1966) and by R/V S.F. Baird (JAPANION, 1961), and the Lamont Doherty Geological Observatory of Columbia University by R/V Vema and by other research vessels (cruise nos. 1007, 1008, 1205, 2106, 2110), and of NAVOCEANO by USNS Silas Bent (OPR. 930001, 1969) and by R/V F. V. Hunt (1969).

3. Lineations

Magnetic anomalies were obtained by subtracting IGRF field (1969) from the observed values. Fig. 2 presents the magnetic anomaly profiles projected on the ship tracks.

In the northern part of the area shown in Fig. 2, the direction of lineations is N65°E. Many authors have reported the direction less than N60°E (e.g. UYEDA *et. al.*, 1968; HILDE *et. al.*, 1975) in the Northwest Pacific Basin. However. N65°E

may be the best fitted direction taking recent data into account (ISEZAKI, 1973; ISEZAKI, in preparation). In the southern part, though there are many seamounts which disturb the lineations as shown in Fig. 3, we can see lineations whose direction is N40°E.

The boundary of direction change, N65°E to N40°E is almost along the latitude of 32°N. The boundary doesn't correspond to evident bathymetric features, but appears to correspond to bathymetric high between 3200-fathom contours and topographic displacement at the southern tip of Shatzky Rise (see Fig. 2; CHASE *et. al.*, 1971). These features seem to belong to some kind of fault but strike slip of a fault alone cannot cause difference of direction of lineations, so 25° anticlockwise rotation of the northern part of the area relative to the southern part by other tectonic mechanism may be expected. The feature seems to extend to the junction of Emperor Seamount Chain and Hawiian Ridge because we can see bathymetric high also

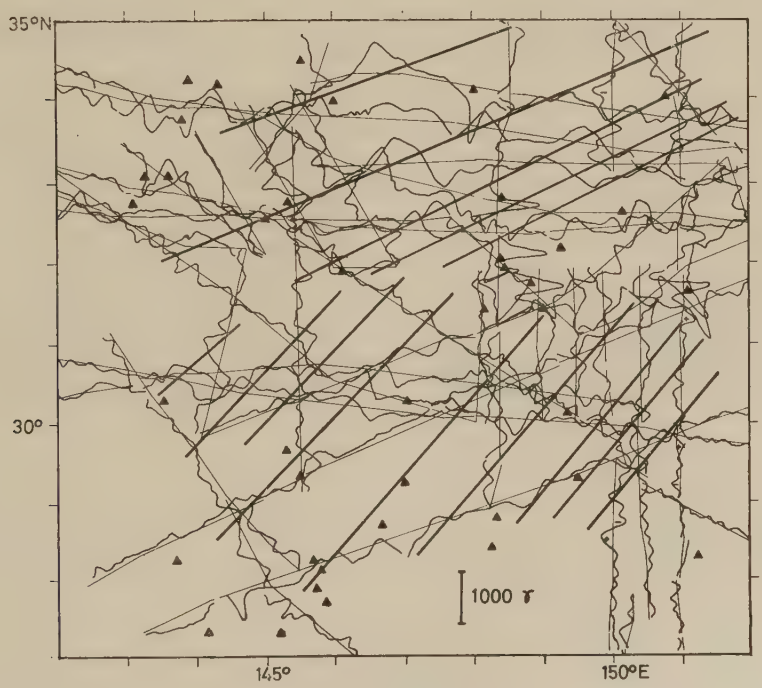

Fig. 2. Magnetic anomaly profiles projected on the tracks. Anomaly in the north side of the track is positive. Identificttions among anomalies are represented by thick solid lines. Note that all discordances in identifications are caused by seamounts represented by triangles.

(Fig. 2) and there also exist two directions of lineations in the area southeast of Shatzky Rise that are N25°W in the northern part of the area and N50°W in the sonthern part (Fig. 3; ISEZAKI in preparation).

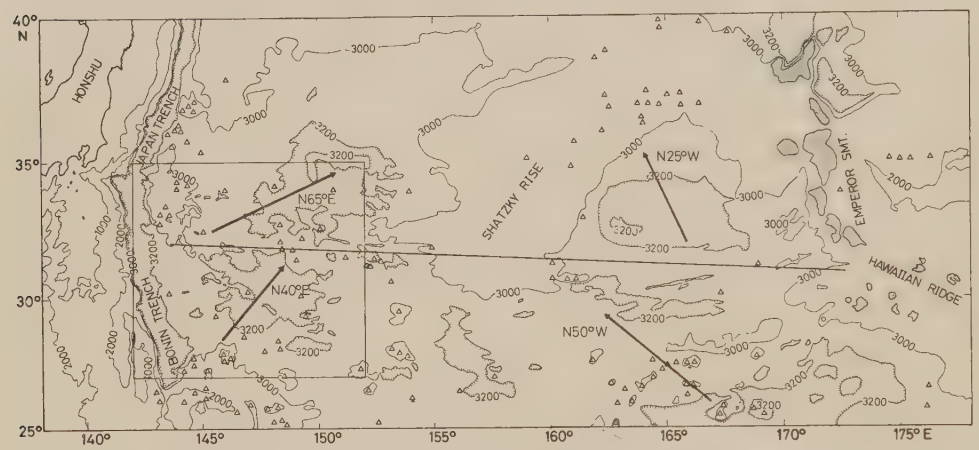

Fig. 3. 3000 and 3200-fathom contours around Shatzky Rise (CHASE et al., 1971). Thick solid line is the boundary mentioned in the text. A square shows the area of which magnetic anomalies are studied in the this paper. Triangles represnt seamouts. Thick arrows shows strikes of anomly linetions.

Though we cannot see the details of the overall magnetic bight by the data available so far, much identifications among anomalies by HILDE *et. al.*, (1975) should be corrected with these new additional data.

Acknowledgements

The author thanks the research staff and crew on board the R/V Ryofu-Maru and Tokaidaigaku Maru II for the work at sea. The author also thanks Dr. Y. KAWARADA of the Meteorolgical College for his kind cooperation in preparing the manuscript.

References

CAHASE, T. E., H. W. MENARD and J. MAMMERIKX (1971): Topography of the North Pacific. *Geologic Data Center, Scripps Institution of Oceanography and Institute of Marine Resources.*

HAYES, D. E. and W. C. PITMAN III (1970): Magnetic lineations in the North Pacific. in J. D. HAYS ed., Geological Investigations of the North Pacific. *Geol. Soc. American Mem.*, **126**, 291–314.

HILDE, T. W. C., N. ISEZAKI and WEGEMAN (1975): Mesozoic seafloor spreading in the North Pacific. *Monogr. Amer. Geophys. Union, Int. Woolard Symp. Volume.* (in press).

IAGA Commission 2 Working Group No. 4 Analysis of the geomagnetic field (1969): The international geomagnetic reference field 1965. 0.

ISEZAKI, N. (1973): Geomagnetic anomalies and tectonics around the Japanese Islands. *Oceanogr. Mag.*, **24**, 107–158.

LARSON, R. L. and C. G. CHASE (1972): Late mesozoic evolution of the western Pacific Ocean. *Geol. Soc. America Bull.*, **83**, 3627–3644.

UYEDA, S., V. VAQUIER, M. YASUI, J. SCLATER, T. SATO, J. LAWSON, T. WATANABE, F. DIXON, E. SILVER, Y. FUKAO, K. SUDO, M. NISHIKAWA and T. TANAKA (1967): Results of geomagnetic survey during the cruise of R/V Argo in western Pasific 1966 and the compilation of magnetic charts of the same area. *Bull. Earthq. Res. Inst. Univ. Tokyo*, **45**, 799–814.

GDP 地磁気観測序報： シャツキーライズの南西海域における地磁気異常

伊勢崎 修弘

（気象大学校）

北西太平洋海盆の地磁気異常の縞模様の方向は，小笠原海溝とシャツキーライズの間の北緯32度付近を境にして，その南北で 150°E から N65°E に変化することが判った。縞模様の方向が変化する境界部には，海底地形の境界がある程度認められ，これがシャツキーライズの上を越えて天皇海山群とハワイ海の嶺のつけねにまで及ぶようにみえる。シャツキーライズの地形からその境界は水平ずれ断層のようにも見えるが，境界の南北で縞模様の方向が異なることから，断層運動ばかりでなく別の造構造運動もこの海域に関与したことが考えられる。

The Oceanographical Magazine
Vol. 27, Nos. 1-2, pp. 43 to 56, March 1976

On the quality control of marine meteorological data practiced in Japan Meteorological Agency

Fumio UEDA
Japan Meteorological Agency
(Received January 24, 1975)

1. Introduction

Meteorological data over open sea are very important not only for improving the accuracy of weather forecast on the real time basis, but also for increasing the accumulation of marine climatological data, which are indispensable for the study of change in the world climate and large scale interaction between air and sea, the exploration of seas, the development of fisheries in the open sea, the planning of safe and economical voyage, etc.

In Japan, marine meteorological data have been compiled and processed for the purposes mentioned above since the first of this century (Imperial Kobe Marine Observatory, 1925–1939, and Japan Meteorological Agency, 1940–1942). In other countries, such as Holland, U.K., U.S.A., U.S.S.R. and West Cermany, similar data compilation have also been done and many useful marine climotological atlases have been published, with different methods of statistics to suit different purposes. In the early fifties, establishment of a new internationally unified system for collection, exchange and statistics of marine meteorological data and the publication of new marine climatological atlases had become desirable in connection with the above-mentioned purposes. In view of these situations, the World Meteorological Organization (WMO) decided to establish a system for collection, exchange, statistics of marine climatological data and publication of marine climatological atlas at its 4th Congress in 1963 (WMO 1956, 1961, 1962 and 1963). By this decision, 9 responsible member countories, Federal Republic of Germany, Hongkong, India, Netherlands, South Africa, U.K., U.S.A., U.S.S.R. and Japan, started to collect marine meteorological data reported from member countries of WMO, to exchange them in the form of the International Maritime Meteorological Punch-Card (Fig. 1) and take statistics of them for their responsible areas retrospectively to 1961. The data thus collected are mostly from weather log books of many kinds of ships, with different instruments and crews who are not always skillful in mete-

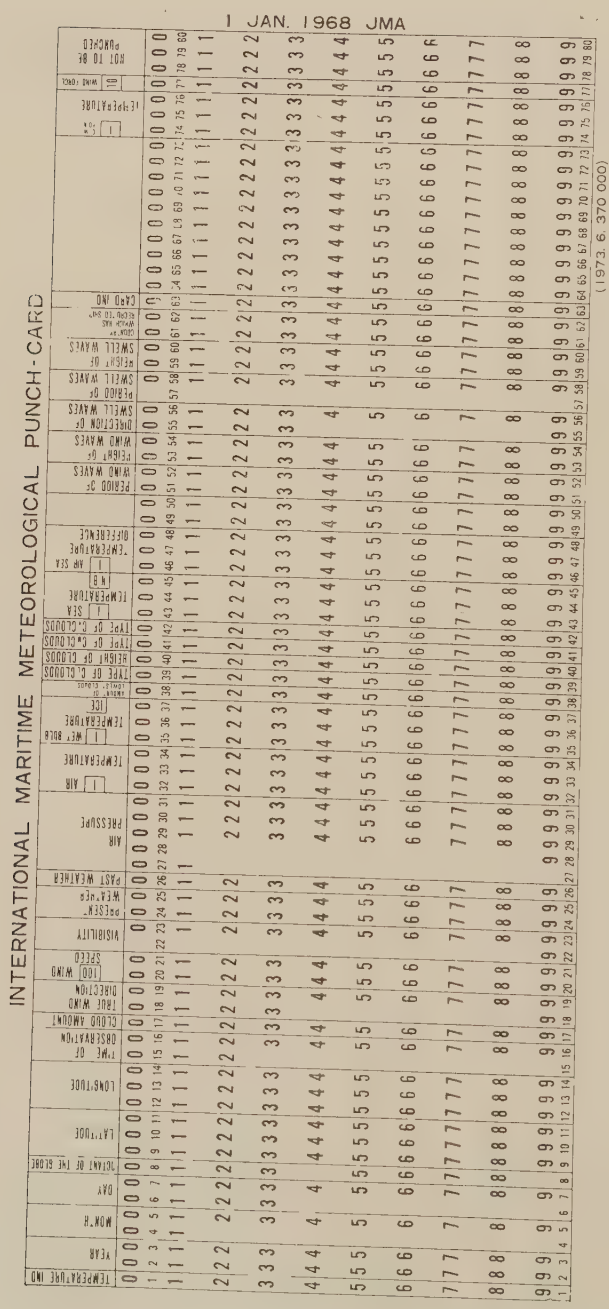

Fig. 1. Form of international maritime meteorological punch-card.

orological observations, so the quality control (QC) of data are especially important and essential. The following are the brief of our system of QC.

2. QC system of JMA

The QC by the Maritime Meteorological Division of the Japan Meteorological Agency (JMA) had been done manually until 1972. The manual QC procedure were troublesome and it took too long a time, and further there remained many overlooked errors. Since a large-sized computer HITAC 8700/8800 system was installed in JMA in October 1974, we could reform the manual QC to the program for the new computer.

2–1. Data sources

Sources of data in Japan are as follows:

(A) marine meteorological observations by WMO voluntary observing ships of Japanese nationality,

(B) those by the research vessels of JMA,

(C) those by the ocean weather station "Tango,"

(D) those by research vessels of the Japanese government other than (B) and (C),

(E) those by foreign ships in the responsible area of Japan, the data of which are sent to JMA in the form of International Maritime Meteorological Punch-Card or magnetic tapes.

2–2. Procedures of the QC

The data from (A), (B), (C) and (D) apply to the manual QC first in the form of log books, the data are punched on punch cards and apply to the automatic QC by electronic computer. The data from (E) are sent to JMA in the form of punched cards or magnetic tapes, so the manual QC is not applied.

Among the errors found by the automatic QC, remediable ones are corrected automatically, and the others are printed out, checked and corrected manually, if possible. After correction and deletion of erroneous elements, the automatic QC is applied to them again. These procedures will be repeated until the errors are exhausted and then the data will be filed on magnetic tapes as the original files. Conversions of the unit necessary for the marine climatological summary will be done for the elements, such as wind speed, air temperature, and so on, and the resultant data will be moved on to magnetic tapes as work files for the summary. In the work files, the data are sorted by month, latitude, longitude, date and time automatically.

2-3. Classification of the QC

We may classify the QC system as follows:

QC
- manual QC
  - serial check
    - correction
    - deletion
  - spatial check
    - correction
    - deletion
  - coding check
    - correction
    - deletion
- automatic QC
  - spatial check
    - correction
    - printing out
  - check other than the serial and spatial checks
    - correction
    - printing out,

where, the serial check means the data from a ship are checked in the time serial order and the spatial check means the data from a ship are checked with the comparison to the other ships or pattern of weather map in the same area.

2-4. Substance of the QC

The contents of the manual and automatic QC are shown in Tables 1 and 2, respectively. In figure 2, block diagrams for checking some elements are shown.

Remarks

The whole QC system of JMA is not complete and there are many points to be improved. In future, serial check will be applied by automatic computer. The spatial check now under way is very simple (air temperature and weather only), so we intend to make spatial check statistically in near future.

References

Imperial Kobe Marine Observatory (1925-1940): The mean atmospheric pressure, cloudness and sea surface temperature, 1911-1939.

Japan Mejeorological Agency (1962): Marine climatological tables of the North Pacific Ocean. Tech. Rep., No. 17.

Japan Meteorological Agency (1963): Marine climatological tables of the North Pacific Ocean. Tech. Rep., No. 23.

World Meteorological Organization (1956): Abridged final report of the 2nd session of Commission for Marine Meteorology.

World Meteorological Organization (1961): Abridged report of the 13th session of the Executive Committee.

World Meteorological Organization (1962): Abridged report of the 14th session of the Executive Committee.

World Meteorological Organization (1963): Abridged report of the 4th Congress.

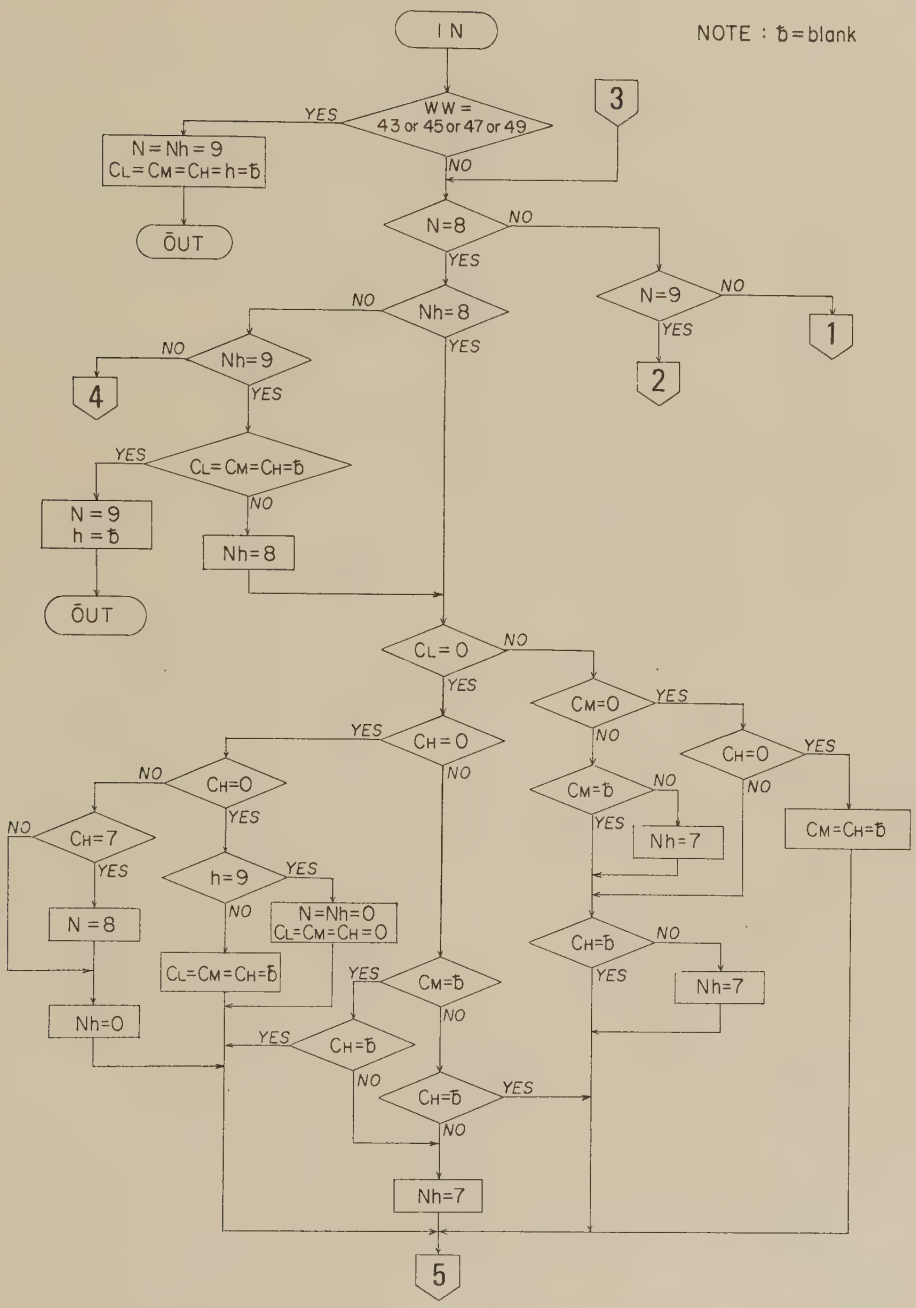

Fig. 2-1. Flow chart of QC for cloud data.

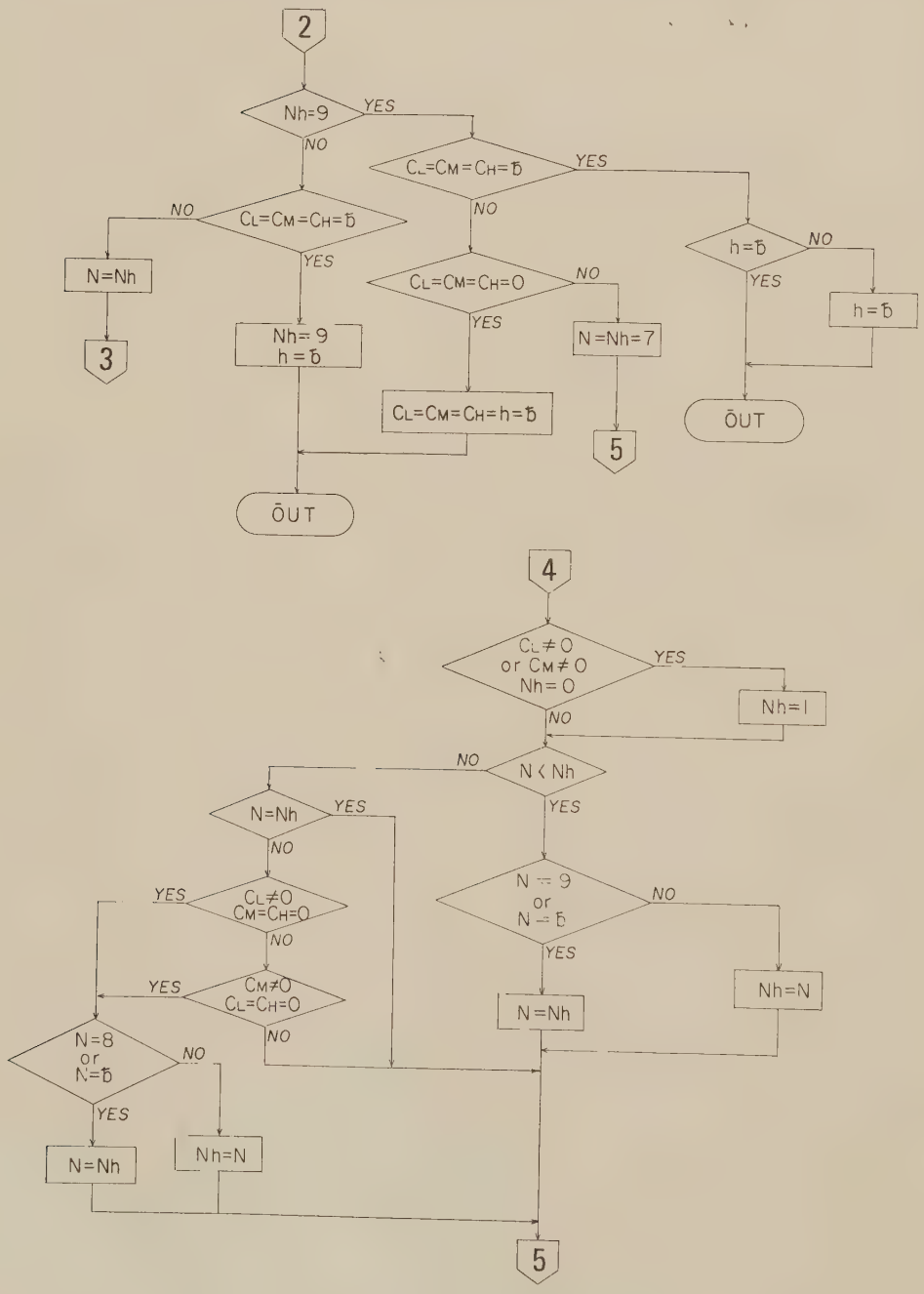
2
Nh=9
YES
NO
CL=CM=CH=5
YES
NO
NO
CL=CM=CH=5
N=Nh
YES
CL=CM=CH=0
NO
h=5
NO
YES
h=5
3
Nh=9
h=5
YES
N=Nh=7
OUT
CL=CM=CH=h=5
5
OUT
4
CL≠0
or CM≠0
Nh=0
YES
Nh=1
NO
NO
N<Nh
N=Nh
YES
YES
NO
N=9
or
N=5
NO
YES
CL≠0
CM=CH=0
YES
NO
CM≠0
CL=CH=0
YES
Nh=N
N=Nh
NO
N=8
or
N=5
NO
YES
N=Nh
Nh=N
5

Fig. 2-2.

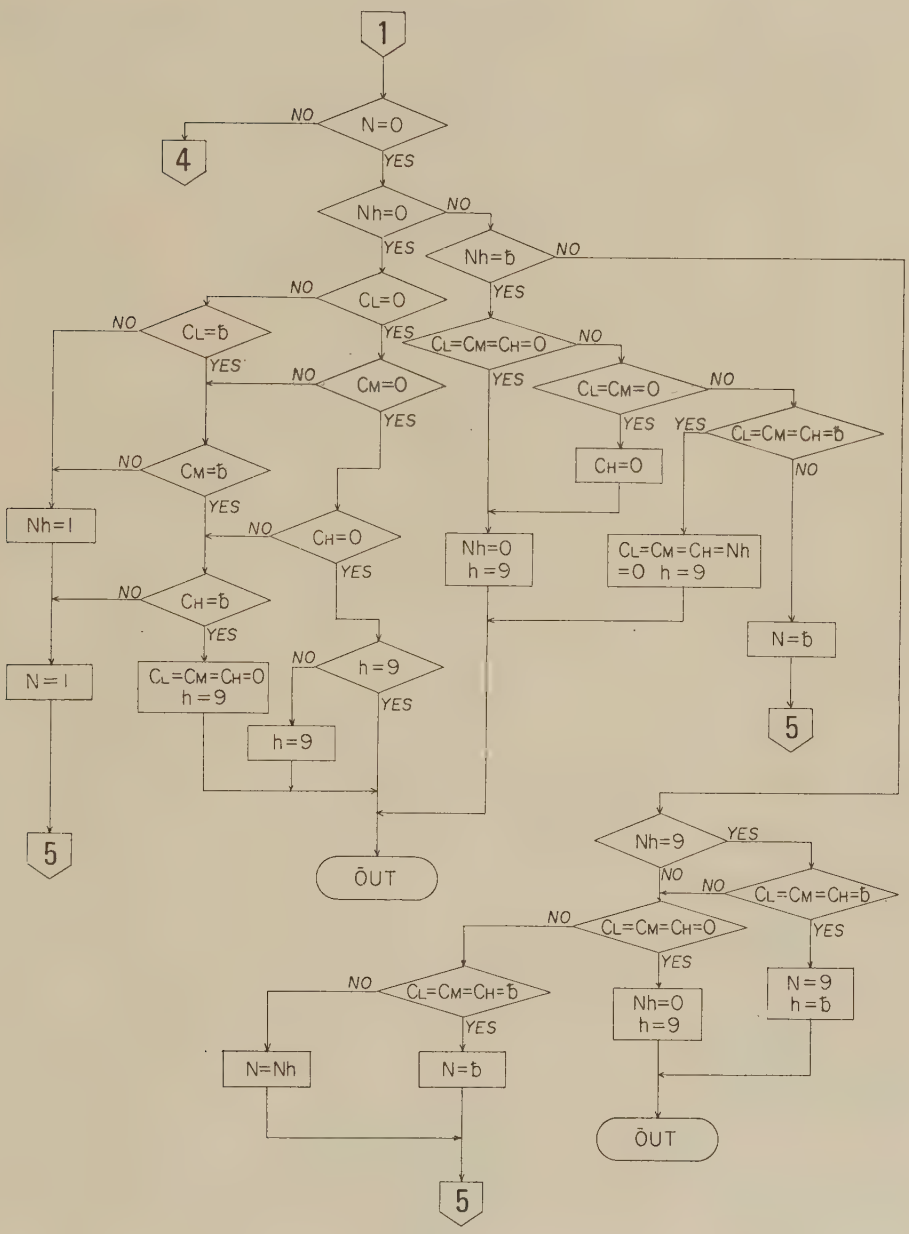
1
N=0
NO
4
YES
Nh=0
NO
YES
Nh=b
NO
YES
CL=0
NO
YES
CL=b
NO
YES
CL=CM=CH=0
NO
YES
CM=0
NO
YES
CL=CM=0
NO
YES
YES
CL=CM=CH=b
NO
CH=0
CM=b
NO
YES
Nh=1
CH=0
NO
YES
Nh=0
h=9
CL=CM=CH=Nh
=0 h=9
CH=b
NO
YES
N=b
5
N=1
CL=CM=CH=0
h=9
h=9
NO
YES
h=9
5
ŌUT
Nh=9
YES
NO
NO
CL=CM=CH=b
NO
CL=CM=CH=0
YES
YES
CL=CM=CH=b
NO
YES
N=9
h=b
Nh=0
h=9
N=Nh
N=b
ŌUT
5

Fig. 2-3.

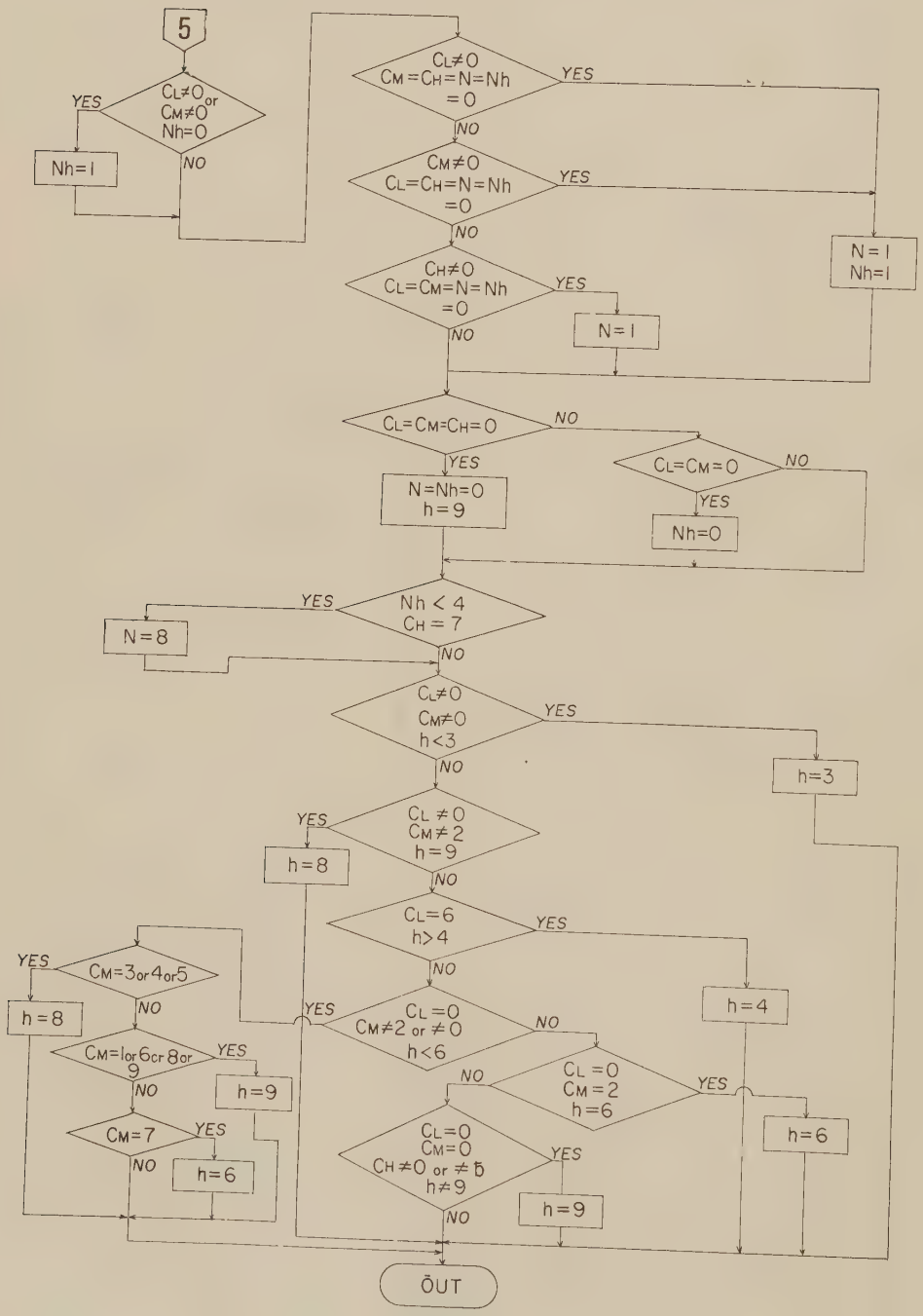
5
CL≠0 or CM≠0 Nh=0
YES
NO
Nh=1
CL≠0 CM=CH=N=Nh =0
YES
NO
CM≠0 CL=CH=N=Nh =0
YES
NO
CH≠0 CL=CM=N=Nh =0
YES
NO
N=1
N=1 Nh=1
CL=CM=CH=0
YES
NO
N=Nh=0 h=9
CL=CM=0
YES
NO
Nh=0
Nh < 4 CH = 7
YES
NO
N=8
CL≠0 CM≠0 h<3
YES
NO
h=3
CL ≠0 CM≠2 h=9
YES
NO
h=8
CL=6 h>4
YES
NO
h=4
CM=3or4or5
YES
NO
h=8
CL=0 CM≠2 or ≠0 h<6
YES
NO
CM=1or6or8or 9
YES
NO
h=9
CL=0 CM=2 h=6
NO
YES
h=6
CM=7
YES
NO
h=6
CL=0 CM=0 CH≠0 or ≠5 h≠9
YES
NO
h=9
OUT

Fig. 2-4.

Table 1. Content of Manual QC

column	element	conditions	dispositions
1	temperature indicator	air temperature and wet-bulb temperature are observed at 1/2°C interval and temperature indicator is not 5	replaced by 5
		air temperature and wet-bulb temperature are observed at 1/10°C interval and temperature indicator is not 1	replaced by 1
		air temperature and wet-bulb temperature are observed at 1°C interval and temperature indicator is not 3	replaced by 3
2, 3	year	indicated by Japanese Era	convert to the Christian Era
		when month changed December to January but year does'nt change	replaced by new year
6, 7	day	the time of observation has changed to 00 but day is the same as the observation just before	replaced by new day
9–11	latitude	changed greatly in a short interval	replaced by the value calculated from the data before and after, or deleted
12–14	longitude	less than 100 degrees	Xoverpunch in column 12*
		changed greatly in a short interval	replaced by the value calculated from the data before and after, or deleted
15, 16	time of the observation	double observations	delete one of it
18, 19	wind direction	wind speed is observed and wind direction is blank	replaced by 99
		greater than 36 (except 99)	correct by the value calculated from the data before and after, or deleted
		changed greatly in a short interval	examine it by weather charts etc., and if the data were incorrect, replaced by the value calculated from the data before and after, or deleted
27–31	air pressure	when less than 1000mb, thousand of mb is not filled in	fill in 0
		blank at thousand and hundred of mb	fill in numbers with reference to weather charts and tens of mb

* domestic procedure

Table 1. continued

column	element	conditions	dispositions
		changed greatly in a short interval	check with weather charts
32-34	air temperature	when below zero, 5 is added to tens of degrees	subtract 5 from tens of degrees and mark (−)
		changed greatly in a short interval	check with weather charts
35-37	wet-bulb temperature	greater than air temperature	check with weather charts
		coding error when below zero	correct
38	N_h	coding error when Nh cannot be estimated	correct
39	C_L	coding error when C_L is unknown	correct
40	h	coding error when h cannot be estimated	correct
41	C_M	coding error when C_M is unknown	correct
42	C_H	coding error when C_H is unknown	correct
43-45	sea-surface temperature	changed greatly in a short interval	check with sea-surface temperature charts
51, 52	period of wind wave	wind wave height is observed and period is blanks	fill with 99
55, 56	swell direction	greater than 36 (except 99)	check with the value before and after
		period and/or height of swell is observed and direction is blanks	fill with 99
58	swell period	filled with whole seconds	fill with the code
59, 60	swell height	swell group is doubled in a same observation time	delete which height is lesser
		changed greatly in a short interval	check
63	card indicator	temperature indicator is 1 and card indicator is not 0	fill with 0*
		temperature indicator is 5 or 3 and card indicator is not 5	fill with 5*
65	wind indicator	wind observed with 36 points, and with knots, and indicator is not zero	fill with 0*
		wind observed with 36 points and with knots by anemometer, and wind indicator is not 6	fill with 6*

* domestic only

Table 2. Content of Automatic QC

column	element	conditions	disposition
1	temperature indicator	the indicator punched is greater than 8, or not punched	print out
		punched 2, 4, 6, 7	temperature are converted °F to °C

Table 2. continued

column	element	conditions	disposition
			and the indicator is converted to 1, 3, 5, 1 respectively
4, 5	month	month punched is greater than 12, or not punched	print out
6, 7	day	day punched is greater than 31 or not punched	print out
8	octant	octant punched 4 or 9 or not punched	print out
9–11	latitude	latitude punched is greater than 901 or not punched	print out
12–14	longitude	octant punched 1, 2, 6 or 7, but longitude punched is except 900–999 and column 12 is X overpunched	print out
		octant punched 1, 2, 6 or 7, but longitude punched 900–999 and column 12 is not X overpunched	print out*
		octant punched 1, 2, 6 or 7, but longitude punched 801–899	print out*
		octant punched 0, 3, 5 or 8, but column 12 is not X-overpunched	print out*
		octant punched 0, 3, 5 or 8, and column 12 is X-overpunched, but longitude punched 900–999.	print out*
15, 16	time of the observation	punched 24	print out
		punched greater than 24	print out
17	total cloud amount	present weather punched 03, 14–17, 19 or 50–99, but cloud amount punched 0 (see table 2 for dispositions of cloud amount)	print out
18, 19	wind direction	wind direction punched greater than 36 (except 99)	print out
		a column not punched	columns leave blank
		wind indicator punched 1, 3, 5, 7, 9	convert to 36 points and the indicator is converted to 0, 2, 4, 6, 8 respectively
		wind speed punched greater than 02, but wind direction punched 00	convert to 36
		wind speed punched 00	convert to 00
		wind direction punched 00, but wind speed punched 01	convert to 99
20, 21	wind speed	wind indiccator punched 4, 5, 8 or 9	convert unit to knots and the indicator is converted to 0, 1, 6, 7 respectively
		wind indicator punched 2 or 3	leave blank**

* domestic only

** Japanese ship do not report by Beaufort scale number

Table 2. continued

column	element	conditions	disposition
22, 23	visibility	visibility punched is not 90–99 (see table 3 for the conversion of visibility)	print out
24, 25	present weather	the amount of low level cloud punched 0, but present weather punched greater than 50 or equal to 50	print out
26	past weather	latitude punched equal to or less than 200, but past weather punched 7	print out
27–31	pressure	air pressure punched less than 8500 or greater than 10700	print out
32–34	air temperature	air temperature punched less than −300 or greater than 400	print out
		present weather punched 22–24, 26, 36–39, 48, 49, 56, 57, 66–79 or 83–86, but air temperature punched greater than or equal to 101	print out
		present weather punched 36–39, 48, 49, 56, 57, 66, 67, 70–79, 85 or 86, but air temperature punched greater than or equal to 041	print out
		latitude punched less than or equal to 200, but air temperature punched less than or equal to 149	print out
		air temperature punched less than wet-bulb temperature	print out
		temperature indicator punched 2, 4, 6 or 7	convert unit from °F to °C, and the indicator is converted to 1, 3, 5, 1 respectively
35–37	wet-bulb temperature	wet-bulb temperature punched less than −100 or greater than 400	print out
		temperature indicator punched 2, 4, 6 or 7	convert unit from °F to °C, and the indicator is converted to 1, 3, 5, 1 respectively
38	the amount of low cloud	(see table 2)	
39	C_L	(see table 2)	
40	h	h=9, but C_L not punched 0 (see table 2 for conversion)	print out
41	C_M	(see table 2)	
42	C_H	(see table 2)	
43–45	sea-surface temperature	sea-surface temperature punched less than −020 or greater than 400	print out
		temperature indicator punched 2, 4, 6 or 7	convert unit from °F to °C, and the indicator is converted to 1, 3, 5, 1 respectively
46–48	air-sea temperature difference	(not to be checked)	

Table 2. continued

column	element	conditions	disposition
49, 50	wind wave direction	wind wave direction punched greater than 36 (except 49 and 99), and the data observed before 1967	print out
		the data observed after 1968	replaced by wind direction
51, 52	wind wave period	the data observed before 1967, and column 51 not punched 0–9, or not blank	print out
		the data observed before 1967, and column 52 is not blank	print out
		the data observed after 1968, and the period punched greater than 30 (except 99) or not blank (see table 4 for the conversion)	print out
53, 54	wind wave height	wind wave height punched greater than 40 or is not blank (see table 5 for the conversion)	print out
55, 56	swell wave direction	swell wave direction punched greater than 36 (except 49 and 99) or not blank	print out
		swell wave period is not blank, but swell wave direction is blank	convert to 99
		swell wave height is not blank, but swell wave direction is blank	convert to 99
		swell wave height and the period is not 00 or not blank, but swell wave direction is 00	convert to 36
57, 58	swell wave period	the data observed after 1968, and column 57 is not blank	print out
		the data observed before 1967, and column 58 is not blank	print out
59, 60	swell wave height	swell wave height punched greater than 40 or is not blank	print out
		swell wave direction punched 00 and the period punched 0, but swell wave height is not 00	print out
63	card indicator	card indicator punched 1, 2, 3, or 4	print out
74–76	dew point temperature	air temperature is equal to wet-bulb temperature	replaced by air temperature
		air temperature is not equal to wet-bulb temperature	table search and disposition

Table 3. Automatic Q.C. for the visibility

conditions	disposition	conditions	disposition
column 23 is blank	let column 22, 23 be blank	ww=10 and VV≧96	VV=95
		ww=11–12 and VV≧94	VV=93
ww=00–03 and VV≦95	VV=96	ww=15 and VV≦95	VV=96
ww=04–05 and VV≧97	VV=96	ww=16 and VV≦93	VV=94
ww=06, 09 and VV≧98	VV=97	ww=16 and VV≧98	VV=97
ww=10 and VV≦93	VV=94	ww=33–35 and VV≧93	VV=92

Table 3. continued

conditions	disposition	conditions	disposition
ww=36 and VV≦92	VV=93	ww=56-63 and VV≧98	VV=97
ww=37 and VV≧93	VV=92	ww=64-65 and VV≧97	VV=96
ww=38 and VV≦92	VV=93	ww=66-73 and VV≧98	VV=97
ww=39 and VV≧93	VV=92	ww=74-75 and VV≧96	VV=95
ww=41-49 and VV≧94	VV=93	ww=76-81 and VV≧98	VV=97
ww=50-53 and VV≧97	VV=96	ww=82 and VV≧96	VV=95
ww=54-55 and VV≧96	VV=95	ww=83-99 and VV≧98	VV=97

Table 4. Automatic Q.C. for the wind wave period

conditions	disposition	conditions	disposition
ff=00 and PwPw≠00 and HwHw≠00	PwPw=00	26≦ff≦35 and PwPw<03	PwPw=03
		36≦ff≦45 and PwPw>18	PwPw=18
00≦ff≦08 and PwPw>04	PwPw=04	36≦ff≦45 and PwPw<04	PwPw=04
09≦ff≦15 and PwPw>08	PwPw=08	46≦ff≦60 and PwPw>24	PwPw=24
09≦ff≦15 and PwPw<01	PwPw=01	46≦ff≦60 and PwPw<06	PwPw=06
16≦ff≦25 and PwPw>10	PwPw=10	ff>60 and PwPw<10	PwPw=10
16≦ff≦25 and PwPw<02	PwPw=02	HwHw≠blank and PwPw=blank	PwPw=99
26≦ff≦35 and PwPw>14	PwPw=14		

(PwPw : wind wave period, HwHw : wind wave height)

Table 5. Automatic Q.C. for the wind wave height

conditions	disposition	conditions	disposition
PwPw=00, or ff=00 and PwPw≠00 and HwHw≠00	HwHw=00	26≦ff≦35 and HwHw>08	HwHw=08
		26≦ff≦35 and HwHw<04	HwHw=04
00≦ff≦08 and HwHw>01	HwHw=01	36≦ff≦45 and HwHw>18	HwHw=18
09≦ff≦15 and HwHw>03	HwHw=03	36≦ff≦45 and HwHw<06	HwHw=06
09≦ff≦15 and HwHw<01	HwHw=01	46≦ff≦60 and HwHw>27	HwHw=27
16≦ff≦25 and HwHw>06	HwHw=06	46≦ff≦60 and HwHw<14	HwHw=14
16≦ff≦25 and HwHw<02	HwHw=02	ff>60 and HwHw<23	HwHw=24

(PwPw : wind wave period, HwHw : wind wave height)

気象庁における海上気象資料の品質管理について

上　田　文　夫
(気象庁海洋気象部)

船舶による気象観測資料について気象庁海上気象課で行なっているデータのチェック等の質管理について述べてある。質管理には電子計算機に行なわせるものと，人間が行なうものがあり，それぞれに適した質管理を行なわせている。

各種のチェック等について気象要素毎に詳しく述べてあり，質管理によって発見された誤りデータの処置方法を記してある。また雲のデータの質管理は複雑なので，フロー・チャートを示した。

気象庁

欧文海洋報告

第 27 巻

TEH

OCEANOGRAPHICAL MAGAZINE

Vol. 27

Published by the Japan Meteorological Agency

March, 1976

CONTENTS

ISOZAKI, I., T. UJI, T. SETO and A. KAIETSU: Ocean waves on Sagami Bay caused by Typhoon 7416 1

NAGASAKA, K.: Direct measurement of deep-sea current by Richardson-type current meters in the western-north Pacific 25

ISEZAKI, N.: A preliminaay report of magnetic survey in GDP; Geomagnetic anomaly lineation in the area southwest of Shatzky rise 37

UEDA, F.: On the quality control of marine meteorological data practiced in Japan Meteorological Agecy 43

昭和51年3月31日　発行

編集兼
発行者　気象庁
東京都千代田区大手町1の3の4

印刷者　藤原秀雄

印刷所　昌美印刷株式会社
東京都千代田区飯田橋2の6の1